

ANALYSIS AND USE OF DISPERSION CURVE FOR CALCULATION OF BEARING CAPACITY

A DISSERTATION

SUBMITTED IN PARTIAL FULFILLMENT OF THE REQUIREMENT
FOR THE AWARD OF THE DEGREE

OF

MASTER OF TECHNOLOGY

IN

GEOTECHNICAL ENGINEERING

Submitted by:

VISHAL SHARMA

(Roll No. 2k19/GTE/18)

Under the supervision of

Prof. A K Shrivastava



DEPARTMENT OF CIVIL ENGINEERING

DELHI TECHNOLOGICAL UNIVERSITY

(Formerly Delhi COLLEGE OF ENGINEERING)

BAWANA ROAD, DELHI-110042)

JULY, 2021

DELHI TECHNOLOGICAL UNIVERSITY
(Formerly Delhi College of Engineering)
Bawana Road, Delhi – 110042

CANDIDATE DECLARATION

I, VISHAL SHARMA, 2k19/GTE/18, student of M.Tech, (Geotechnical Engineering), hereby declare that the Major project II Dissertation titled “ANALYSIS AND USE OF DISPERSION CURVE FOR CALCULATION OF BEARING CAPACITY” which is submitted by me to the Department of Civil Engineering, Delhi Technological University, Delhi in partial fulfilment of the requirement of the marks of award degree of Master of Technology is original and not copied from any source without proper citation. This work has not previously formed the basis for the award of any Degree, Diploma Associateship, Fellowship or other similar title or recognition.

Place: Delhi

VISHAL SHARMA

Date: 18th July 2021

DEPARTMENT OF CIVIL ENGINEERING
DELHI TECHNOLOGICAL UNIVERSITY

(Formerly Delhi College of Engineering)

Bawana Road, Delhi-110042

CERTIFICATE

I hereby certify that the major project II titled “ANALYSIS AND USE OF DISPERSION CURVE FOR CALCULATION OF BEARING CAPACITY” which is submitted by me **VISHAL SHARMA (2K19/GTE/18)** belonging to Master of Technology, Geotechnical engineering, Civil Engineering Department, Delhi Technological University, Delhi in partial fulfilment of the requirement for the award of Master of Technology is a record of the project work carried out by the students under my supervision. To the best of my knowledge, this work has not been submitted in part or full for any Degree or Diploma to this University or elsewhere.

Place: Delhi

Date: 18th July 2021

Prof.A.K Shrivastava

SUPERVISOR

ACKNOWLEDGEMENT

I would like to express heartfelt gratitude to my esteemed supervisor Prof. A.K Shrivastava for his encouragement, direction, support and consistent backing throughout the course of my work. I genuinely acknowledge his faith in me and his continuous support from start to the end of this research work.

I would also like to extend my earnest gratitude towards Prof V K Minocha, HOD, Civil Engineering Department, Delhi Technological University, who have illuminated me all through my research work. I am also thankful to all the faculty members of the Civil Engineering Department, who were there and helped me directly or indirectly in my research work.

A noteworthy gratitude to Mr. Shubham Gupta, M.tech. student of Civil Engineering Department, Delhi Technological University for his help, support, support throughout my research work.

Finally, I would like to thank my family members and friends for their moral support, encouragement who stood with me through thick and thin, without them it was not possible.

VISHAL SHARMA

Roll No. 2k19/GTE/18

M.Tech (Geotechnical Engineering)

Department of Civil Engineering

Delhi Technological University

ABSTRACT

Liquefaction of soil is one of the major factor of the failure of structures, occurring in the loose saturated sand deposits due to generation of excess pore water pressure. This pore water pressure generates when external shaking like earthquake forces are applied on the soil mass. Although the prevention of this phenomenon can be done by proper soil investigation and analysis. In this study empirical formulas are used for the assessment of liquefaction potential of the soil locally available at Delhi Technological University. SPT 'N' values, obtained from DTU soil report have taken for the analysis. Along with that the bearing capacity analysis is carried out using shear wave velocity and obtained results are compared with classical approach results. The shear wave velocity of the soil is evaluated using Multichannel Analysis of Surface Wave (MASW), which is the seismic technique to evaluate the shear wave velocity. Geophones are used for picking up seismic energy coming from active source. These energies are converted into the dispersion curve from where shear wave velocity evaluation along the depth is carried out using Winmasw software. The shear wave velocity is evaluated for four different locations of DTU. After getting adequate shear wave velocity values for these location allowable bearing capacity has been calculated by an empirical formula. Approach using seismic wave velocity is useful in saving the time and cost. Results shows the average shear wave velocity for the Delhi Technological area has found to be nearly to 300 m/s. This comparative study of evaluation of allowable bearing by using shear wave velocity with the classical Terzaghi approach showed that the alteration in allowable bearing capacity has found in very nominal range at these four specific location. Factor of safety from different analytical methods are presented, showing the difference in FOS value at various depth due to change in formulation of CSR (cyclic resistance ratio) and CRR (cyclic resistance ratio).

TABLE OF CONTENTS

| | |
|--|------|
| Candidate's Declaration | i |
| Certificate | ii |
| Acknowledgement | iii |
| Abstract | iv |
| List of Tables | vii |
| List of Figures | viii |
| List Symbols and Abbreviations | x |
| | |
| CHAPTER 1 | |
| 1.1 Introduction | 1 |
| 1.2 Objective of Thesis | 2 |
| 1.3 Methodology Adopted | 3 |
| | |
| CHAPTER 2 | |
| 2.1 Literature Review | 4 |
| 2.1.1 Liquefaction Susceptibility Analysis | 5 |
| 2.2 Use of Shear Wave Velocity | 6 |
| | |
| CHAPTER 3 | |
| 3.1 Liquefaction Potential Analysis | 8 |
| 3.1.1 Liquefaction potential assessment analytical solutions | 8 |
| 3.2 Graphical analysis of liquefaction susceptibility | 12 |
| | |
| CHAPTER 4 | |
| 4.1 Methodology Adopted To Calculate Vs | 14 |
| 4.2 Types of Seismic Waves | 14 |
| 4.2.1 Body Waves | 14 |
| 4.2.2 Surface Waves | 16 |
| 4.3 Instrument Setup | 17 |
| 4.3.1 Seismograph | 17 |

| | |
|---|----|
| 4.3.2 Geophone | 18 |
| 4.3.3 Sledge Hammer | 19 |
| 4.3.4 Location of MASW Testing | 20 |
| 4.4 Data Acquisition and Analysis | 21 |
| 4.4.1 Analysis of Data | 23 |
| CHAPTER 5 | |
| 5.1 Classic Approach | 25 |
| 5.2 Approximation Made in Classical Method | 27 |
| 5.2.1 Practical Guideline | 28 |
| 5.3 Allowable Bearing Capacity by Shear Wave Velocity | 29 |
| 5.3.1 For the Purpose of Settlement Control | 29 |
| 5.3.2 For Setting an Upper Limit for q_a | 32 |
| 5.4 To Determine Unit Weight | 33 |
| CHAPTER 6 | |
| 6.1 Evaluation of Allowable Bearing Capacity | 34 |
| 6.2 Using of Classical Method to Calculate Allowable Bearing Capacity | 34 |
| 6.3 Use V_s to Evaluate Allowable Bearing Capacity | 36 |
| CHAPTER 7 | |
| 7.1 Conclusion | 37 |
| REFERENCES | |

LIST OF TABLES

| | |
|--|----|
| Table 3.1 Obtained FOS from different analytical methods | 14 |
| Table 4.1 Shows the technical specifications of the instrument GEA24 used | 18 |
| Table 4.2 Geophone frequency and their possible investigation depth. | 19 |
| Table 4.3 Calculated Shear Wave Velocity Vs30 | 21 |
| Table 5.1 Allowable bearing capacities (KPa) variation for different soil type | 29 |
| Table 5.2 Locations of various case study with their allowable bearing capacity | 31 |

LIST OF FIGURES

| | |
|--|----|
| Fig 1.1 Bearing capacity failures cause due to Liquefaction Niigate earthquake | 2 |
| Fig 1.2 Flow chart of MASW Seismic Method | 3 |
| Fig 2.1 Relation between Epicentral Distance and Magnitude | 4 |
| Fig 2.2 SPT based Liquefaction Generating Curves | 5 |
| Fig 3.1 Depth and factor of safety by T.L Youd and I.M IDRIS based on SPT 'N' Values | 12 |
| Fig 3.2 Depth V/s factor of safety by IS Code 1893 (Part 1):2016 based on SPT 'N' Values | 12 |
| Fig 3.3 Depth V/s factor of safety by I. M. IDRIS and R. W. BOULANGER based on SPT 'N' Values | 13 |
| Fig 4.1 Propagation of Primary/Compressional Wave | 15 |
| Fig 4.2 Propagation of Secondary/Shear Wave | 16 |
| Fig 4.3 Propagation of Love Wave | 16 |
| Fig 4.4 Propagation of Rayleigh Wave | 17 |
| Fig 4.5 Seismograph | 18 |
| Fig 4.6 Geophones | 19 |
| Fig 4.7 Sledge Hammer | 20 |
| Fig 4.8 Location of MASW Testing | 21 |
| Fig 4.9 Calculated Shear Wave Velocity Vs30 | 21 |
| Fig 4.10 Location 3 Velocity Profile | 22 |
| Fig 4.11 Location 2 Velocity Profile | 22 |
| Fig 4.12 Location 1 Velocity Profile | 22 |
| Fig 4.13 Location 4 Velocity Profile | 22 |

| | |
|--|----|
| Fig 4.14 Location 1 Seismic Data | 23 |
| Fig 4.15 Location 3 Seismic Data | 23 |
| Fig 4.16 Location 1 Dispersion Curve | 24 |
| Fig 4.17 Location 3 Dispersion Curve | 24 |
| Fig 5.1 Zones of Plastic equilibrium | 25 |
| Fig 5.2 Modes of failure | 26 |
| Fig 5.3 Allowable bearing capacity of soils relation with V_s | 32 |
| Fig 5.4 Unit weight relation to V_p | 33 |
| Fig 6.1 Allowable bearing capacity for Location 4 | 35 |
| Fig 6.2 Allowable bearing capacity for Location 1 | 35 |
| Fig 6.3 Allowable bearing capacity for Location 2 | 36 |
| Fig 6.4 Allowable bearing capacity for Location 3 | 37 |

LIST OF SYMBOLS, ABBREVIATIONS

| | |
|-------|--|
| SPT | Standard Penetration Test |
| MASW | Multichannel Analysis of Surface Waves |
| CPT | Cone Penetration Test |
| V_s | Shear Wave Velocity |
| SASW | Spectral Analysis of Surface Waves |
| HVSR | Horizontal/Vertical Spectral Ratio |
| q_u | Ultimate Bearing Capacity |

CHAPTER 1

1.1 INTRODUCTION

Liquefaction in soil is a process due to which soil loses its strength and rigidity during the seismic disturbances cause a serious destruction. As a geotechnical investigator it is must to check the soil liquefaction susceptibility. Liquefaction occurred in loose saturated cohesionless soil during the earthquakes is responsible for structural failure and destruction to roads, pipe-line, and buildings etc. Liquefaction occurs most frequently near rivers, the sea, and water bodies. The term flow failure is a type of liquefaction happen when the soil strength reduced below up to that level which is needed to keep the stability under static condition. Destruction of foundation by reducing the bearing capacity, slopes cause due to the flow failures which is generated by gravitational forces (Figure 1.1) Kramer (1996).

The soil liquefaction susceptibility based on the diverse types of parameters which are magnitude of earthquake, relative density of soil, grain size distribution, fine content, plasticity index of fines, distance from earthquake source, typical site situations, ground acceleration, kind of strata and soil layer thickness, fluctuation of ground water level and decrease of effective stress. The best common technique which is using in engineering exercise for the evaluation of liquefaction susceptibility for sands and silts is the simplified process. This approach can be utilised with either blow counts from a standard penetration test (SPT), cone tip resistance from a cone penetration test (CPT), or by shear wave velocity (V_s) detected within the soil. We have different seismic methods to calculate shear wave velocity, for example SASW, MASW, HVSR etc.

By evaluation of V_s we can find different soil properties for example, the ultimate bearing capacity ' q_u ' of a shallow foundation is one of the essential features of soil that must be determined before any structure may be built on it. (Prandtl, 1921) and (Reissner, 1924) used for the first time in 1921, the idea of plastic equilibrium was used to study under a shallow foundation bearing capacity of an individual soil. However, the formula was

somewhat altered and afterwards reorganised by different researchers “ (Terzaghi, 1925), (Meyerhof, 1956), (Hansen, 1968) and (DeBeer, 1970) and (Sieffert, 2000).



Figure 1.1 Bearing capacity failures cause due to liquefaction of the Kawagishi-cho apartment building following the 1964 Niigata earthquake.

1.2 Objectives of Thesis

1. To study different method of analysis for liquefaction potential assessment and obtaining the factors affecting the result for each method.
2. To evaluate the shear wave velocity at four different locations in Delhi Technological University using Multichannel Analysis of Surface Wave (MASW).
3. Evaluation of Bearing capacity of soil using shear wave velocity and IS Code, comparing the results obtained from both approaches.

1.3 Methodology adopted

1. Here MASW seismic method have used to accumulate the data at site to get the surface wave analysis flow chart shows the process of MASW data acquisition as mentioned below fig 1.2.

2. We have used active acquisitions system in which aluminium plate and sledge hammer was used to generate the surface waves.
3. For geotechnical surface wave studies, vertically polarised Rayleigh waves are maintained in attention.
4. Improper extraction of dispersion curve will give incorrect values of V_s so it is very important step to pick the correct frequency on the dispersion to get the correct result.

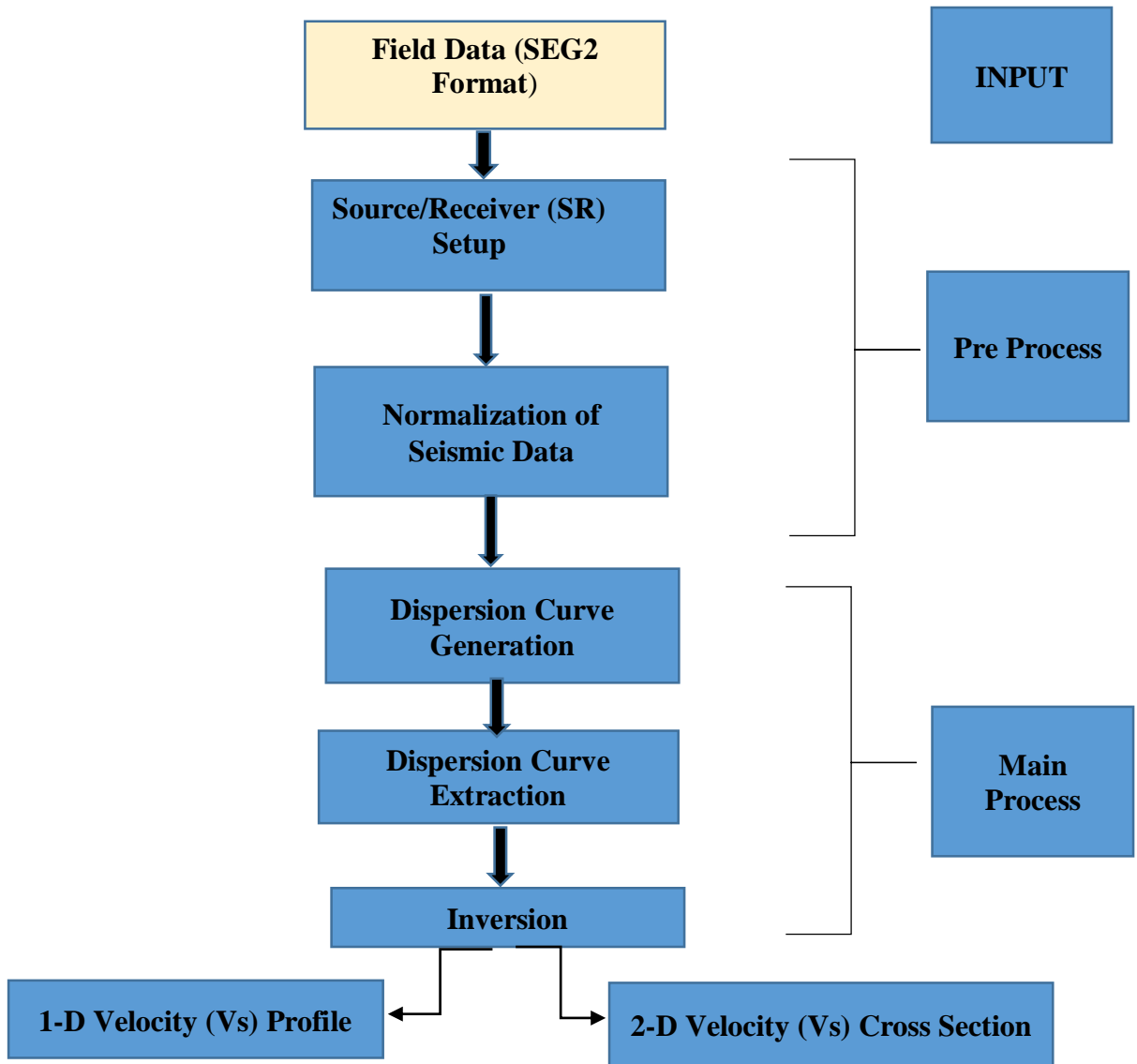


Figure 1.2 Flow Chart of MASW Seismic Method

CHAPTER 2

2.1 Literature Review

The study of liquefaction and its susceptibility have already done by different researcher also helpful for its reduction method. Present study gives the idea of how liquefaction potential can calculate by N values also calculated by Vs values. Liquefaction One of the most dangerous components of an earthquake is induced ground failure. Strong ground shaking causes pore water pressure to build up in saturated unconsolidated soils. If the induced shear stains are large enough and last long enough, the pore water pressure can reach or exceed the value of overburden pressure, resulting in shear strength loss or soil failure (Seed and Idriss, 1971). Lots of researcher have done many study to reduce the effect of liquefaction in loose saturated sand and correlate with the seismic disturbances e.g. earthquake. In fig 2.1 correlation between the earthquake magnitude with the site of liquefaction in terms of epicenter distance of earthquake is given by Kuribayashi and Tatsuoka (1975).

$$\text{Log } R_e = 0.77M - 3.6 \tag{2.1}$$

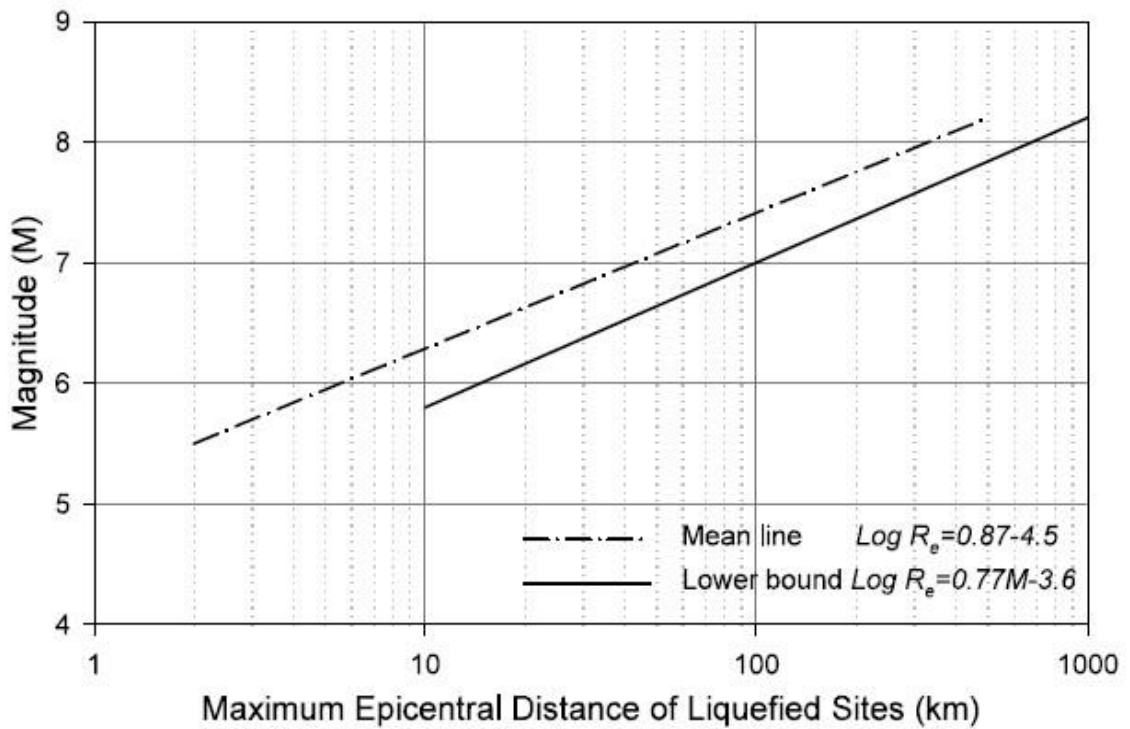


Fig 2.1 Relation Between Epicentral Distance and Magnitude Kuribayashi (1975)

Here, R_e is the epicenter distance of the liquefaction site (Km) and M shows the magnitude of earthquake.

2.1.1 Liquefaction Susceptibility Analysis

The results of a reorganized SPT-based liquefaction generating mechanisms were reported by Idriss and Boulanger (2010). The update of the case history record was part of the reassessment. They sought to figure out what was causing the discrepancies in the liquefaction generating relationships provided by Professor H. Bolton Seed and colleagues (Seed et al., 1984:1985), which were used at the NCEER/NSF workshops with minor alterations (Youd et al., 2001), and those published more lately by Cetin et al. (2004) and Idriss and Boulanger (2004,2008). In fig. 2.2, these liquefaction generating correlations are compared to $(N_1)_{60CS}$ using the cyclic resistance ratio (CRR) adjusted for $M = 7.5$ and $\sigma'v = 1$ atm.

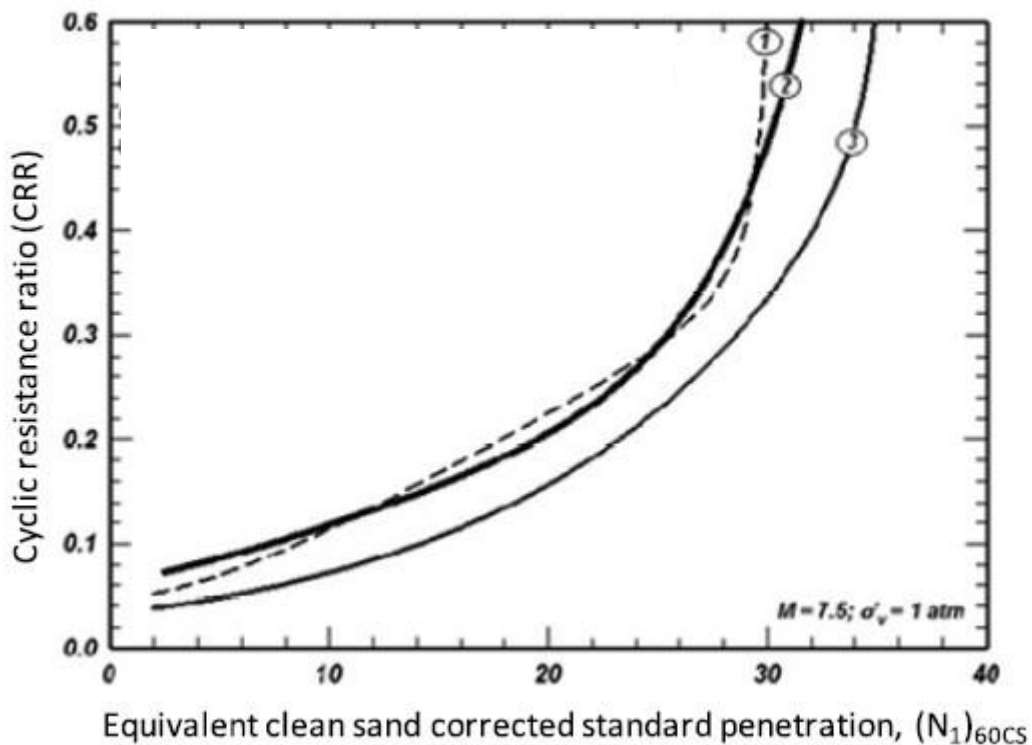


Fig 2.2 SPT based Liquefaction Generating Curves 1. Seed (1984), 2. Idriss and Boulanger (2004), 3. Cetin (2004)

Researchers have done study to find the different parameter on which liquefaction potential depends like magnitude scaling factor, Idriss and Boulanger (2008) proposed a new MSF relationship based on (1) a laboratory-based relationship between the CRR and

the number of loading sequences. (2) The link between loading cycles and earthquake magnitude. Idriss (1999) developed the MSF for sands, which Idriss and Boulanger (2008) used to derive the following equation:

$$\text{MSF} = 6.9 \cdot \exp\left(\frac{-M}{4}\right) - 0.058 \leq 1.8 \quad (2.2)$$

Study of Liquefaction have been common in every soil investigation easily calculated by seismic evaluation. Liquefaction susceptibility also evaluate by Vs values which is easily calculated by different seismic method, Park et al. (1999) reported that by using ground roll recorded on a single short gather, a highly precise dispersion curve may be obtained and inverted to give a, V-s. profile with high assurance and uniformity. During the data collecting and processing step, the reliability of each individual Rayleigh wave frequency may be easily evaluated for defilement by apparent noise, allowing changes to increase the S/N ratio.

2.2 Use of Shear Wave Velocity

Many researcher carry out various case study and gave direct empirical relation by which we can evaluate Semih S. Tezcan (2006) (Tezcan, 2006) presented an empirical method for determining shallow foundations' allowed bearing capacity q_a . by calculated transverse shear wave velocity and the weight density. The foundation size and depth are not taken into account in the shear wave velocity technique. An important single field value, the in-situ evaluated shear wave velocity V_s , is capable of showing true soil conditions at the site factors such as water content, relative density, void ratio, non-uniformity, and compressive strength.

Researcher also have found V_s values very useful to calculate the various soil properties, Semih S. Tezcan (2009) gave the empirical relation for young's modulus of elasticity E , bulk modulus, Poisson's ratio μ , coefficient of subgrade reaction, oedometric modulus related to v_p and v_s only . Above than 373 case studies showed that the results accomplished using the seismic method are more steady, constant, and accurate than those obtained using the conservative method.

Present study idea has taken the idea with the help of a presented paper, Rajat et. al (2020) They have performed the masw seismic test on DTU soil at six different site. By taken seismic data from site made different velocity inversion curve with depth and verify with

NEHRP (National Earthquake Hazard Reduction Programme) site classification system. They have seen the average shear wave velocity of delhi technological university, ground test site is 285 m/s. Which indicate that the area of study falls under the site class D according to NEHRP site class.

Researcher have found the wavelength of surface waves varies with deep layer frequency Long wavelengths penetrate deeper levels and are more sensitive to the elasticity of the deeper layers. Longer wavelengths are associated with faster phase velocities. Because shorter wavelengths are more sensitive to the physical properties of the surface layers, a particular mode of surface wave will have a unique phase velocity for each wavelength, resulting in seismic signal dispersion (Xia et al., 1999).

Many researchers have found Rayleigh waves have similar behavior as waves generate during earthquake, Rayleigh waves travel as different modes, with a mode being a 'packet' of sound energy that propagates in one direction while confined in the other two directions. Rayleigh waves are restrained to the earth-air interface because they are surface waves (Duffy,2008). Therefor as stated above an individual type of Rayleigh wave will have a particular transmission velocity for a given frequency. By these modes, fundamental mode Rayleigh-waves, which travel in an anticlockwise motion, are the slowest and so appear closer to the origin in a frequency versus phase velocity plot. This is called a dispersion plot.

Researcher have found the MASW which can be done by various ways according to their need. MASW seismic survey are of three types 1) Active source MASW, in which seismic data is gathered by impact triggered 2) Passive source MASW, in which disturbances measured for a long time without using an active source (Park and Miller, 2006); and 3) Passageway active source MASW in which 2-5 shot records are gathered to make coherent records by keeping either source or receiver fixed (Vincent et al., 2006).

CHAPTER 3

3.1 Liquefaction Potential Analysis

The creation of an analytical structure to organise previous case study experiences, as well as the creation of an appropriate in-situ index to describe soil liquefaction features, are two key elements of semi empirical field based approaches for assessing liquefaction potential during earthquakes. The original simple approach for estimating earthquake-induced cyclic shear stresses (Seed and Idriss 1971) is still useful. Although the various components of this framework have undergone a lot of improvements, it remains an important component of the analytic framework. In the last thirty years, in-situ index tests (e.g., SPT, CPT, BPT, shear wave velocity) have improved, as has the continued collection of liquefaction/non-liquefaction case histories.

This work presents an update on semi-empirical field-based methodologies for assessing cohesionless soils' liquefaction potential during earthquakes. The stress reduction coefficient, the r_d magnitude scaling factor, the MSF overburden correction factor for cyclic stress K ratios, and the overburden correction factor for penetration CN resistances are all recommended relations in this update. The emphasis has been on constructing relationships that capture the underlying physics while being as simple as possible for each of these parameters. Rechecked of the practical case studies yielded these enhanced deterministic SPT-based and CPT-based liquefaction correlations. Finally, the processes for evaluating the cyclic loading behaviour of plastic fine-grained soils using shear wave velocity VS based liquefaction correlations and VS the procedures for evaluating the cyclic loading behavior of plastic fine-grained soils are briefly reviewed.

3.1.1 Assessment of Liquefaction Potential Analytical Solutions

Because it is difficult to gather and test the (UDS) undisturbed samples from the area which is prone to liquefaction, testing at site is best way to for determining a soil deposit's liquefaction potential. Liquefaction potential calculation methods such as SPT as well as CPT are routinely used in practice. The simplified process is the most popular method for calculating the liquefaction susceptibility for the soil type of loose sands and silts in engineering practise. The methodology can be utilised using three different types which are:

- 1) No of blows count by field standard penetration test (SPT)
- 2) A tip resistance value by a cone penetration test (CPT)
- 3) shear wave velocity V_s estimated within the soil

Step 1 - The water position, SPT value i.e. blow count N or tip of resistance q_c of a CPT cone, unit weight density, and percentage of soil fines content are all needed to determine liquefaction potential.

Step 2 - Evaluate total normal overburden stress σ and effective normal overburden stress' at different depths for all potentially liquefiable layers within the deposit.

Step 3 - Assess the stress reduction factor r_d by applying the following criteria:

$$r_d = \begin{cases} 1-0.00765z & 0 < z \leq 9.15 \text{ m} \\ 1.174-0.0267z & 9.15\text{m} < z \leq 23 \text{ m} \end{cases} \quad (3.1)$$

Here z denotes the depth below the ground in meter.

Step 4- Evaluation of cyclic stress ratio due to earthquake will be find by this formula:

$$CSR = 0.65 \left(\frac{a_{max}}{g} \right) \left(\frac{\sigma}{\sigma'} \right) \quad (3.2)$$

Here

a_{max} =ultimate ground acceleration

g = acceleration caused by gravity and

r_d = factor for stress reduction

if this r_d factor is not available then we take the ratio of (a_{max}/g) equal to seismic factor Z .

Step 5- Correct the standard cycle resistance ratio $CRR_{7.5}$ which is due to earthquake magnitude, more overburden pressure level, and more starting static shear stress to find the cyclic resistance ratio CRR .

$$CRR = CRR_{7.5} (MSF)K_{\sigma}K_{\alpha} \quad (3.3)$$

Here, $CRR_{7.5}$ = For a 7.5 magnitude earthquake. SPT N value, CPT q_c value, or shear wave velocity V_s were used for determine the standard cyclic resistance ratio in the following step and MSF = The magnitude scaling factor is derived using the equation below:

$$MSF = 10^{2.24} / M_w^{2.56} \quad (3.4)$$

MSF factor is used only when the earthquake magnitude is different from 7.5. ($K\sigma$) an improvement factor is used for overburden stress when it is more than (depth > 15 m) and calculated by the equation given below:

$$K_\sigma = (\sigma' / P_a)^{(f-1)} \quad (3.5)$$

Here P_a = atmospheric pressure, σ' = effective overburden compression will be calculated in same units. f is used as an exponent and its value rely on the relative density of soil (D_r). For $D_r = 40\% - 60\%$, f will be 0.7 - 0.8 and for $D_r = 60\% - 80\%$, f will be 0.6 - 0.7. $K\alpha$ factor is used only for the ground which is not plane i.e slope ground it is used for static shear stress generally not used in common engineering purpose hence the value of $K\alpha$ can be taken 1.

To determine liquefaction susceptibility by method given in step 6:

Step 6 – Evaluate cyclic resistance ratio $CRR_{7.5}$

- I. By values of SPT blows;
- II. Calculate the SPT N_{60} value, where 60 is the hammer efficiency of 60 percent. Table 11 has the Provisions for standard equipment. When the equipment will be of non – standard type, N_{60} should be calculated by the observed value of(N);

$$N_{60} = N C_{60} \quad (3.6)$$

Here,

$$C_{60} = C_{HT} C_{HW} C_{SS} C_{RL} C_{BD} \quad (3.7)$$

Factors C_{HT} , C_{HW} , C_{SS} , C_{RL} and C_{BD} has been given by researchers for justify the non-standard SPT procedures are represent in TABLE 12. SPT performed as per IS Code 2131. The energy transferred to drill rod is approximately 60 % because of this , C_{60} can be taken as 1. The computed N_{60} is regularized to an effective overburden compression of about 100 kpa by overburden correction factor C_N given below:

$$(N_1)_{60} = C_N N_{60} \quad (3.8)$$

Here,

$$C_N = \sqrt{\frac{p_a}{\sigma'}} \leq 1.7 \quad (3.9)$$

To show the effect of fines content FC (in %) can be reasonably showed by modified $(N_1)_{60}$ and $(N_1)_{60CS}$ can be found by below formula:

$$(N_1)_{60CS} = \alpha + \beta(N_1)_{60} \quad (3.10)$$

Here,

$$\begin{aligned} \alpha = 0 & \quad \beta = 1 & \quad \text{for FC} \leq 5\% \\ \alpha = e^{\left[1.76 \left(\frac{190}{FC^2}\right)\right]} & \quad \beta = 0.99 + \frac{FC^{1.5}}{1000} & \quad \text{for } 5\% < FC < 35\% \\ \alpha = 0.5 & \quad \beta = 1.2 & \quad \text{for FC} \geq 35\% \end{aligned} \quad (3.11)$$

After that fig 8 may be utilised to evaluate $CRR_{7.5}$, where $(N_1)_{60CS}$ may be used instead of $(N_1)_{60}$ and only SPT sand curve will be utilised regardless of fines contents. The $CRR_{7.5}$ should be assessed using following equation rather of fig 8:

$$CRR_{7.5} = \frac{1}{34 - (N_1)_{60CS}} + \frac{(N_1)_{60CS}}{135} + \frac{50}{[10 \times (N_1)_{60CS} + 45]^2} - \frac{1}{200} \quad (3.12)$$

Step 7- Evaluate the factor of safety FS for find liquefaction susceptibility:

$$FS = \frac{CRR}{CSR} \quad (3.13)$$

Where CSR was evaluated in step 4 and CRR was evaluated in step 5. When the proposal ground signal is conventional, earthquake related perpetual ground distortion will normally be small, if Factor of safety $FS \geq 1.2$.

Step 8- If Factor of safety is less than 1, Then soil tested is expected to liquefiable.

3.2 Graphical Analysis of Liquefaction Susceptibility

Below graph shows the comparative study between different analytical approach to evaluate liquefaction potential.

We have found that graphically that the values for factor of safety vs depth to evaluate liquefaction potential given by three Analytical methods are getting different as presented in fig 3.1 to 3.3, because of following formulation difference in these three methods described below:

- (1) In Idriss and Boulanger (2010) Analytical method shows that the soil is liquefiable with depth at some points because in this method to calculate CRR (Cyclic Resistance Ratio) the formula is based upon different power of N_{160cs} and also the different value of Stress Reduction factor r_d used in this method.
- (2) In IS Code 1893 (Part1):2016 and Youd and Idriss (2001) the difference in factor of safety is due to different formulation method for MSF (magnitude scaling factor).

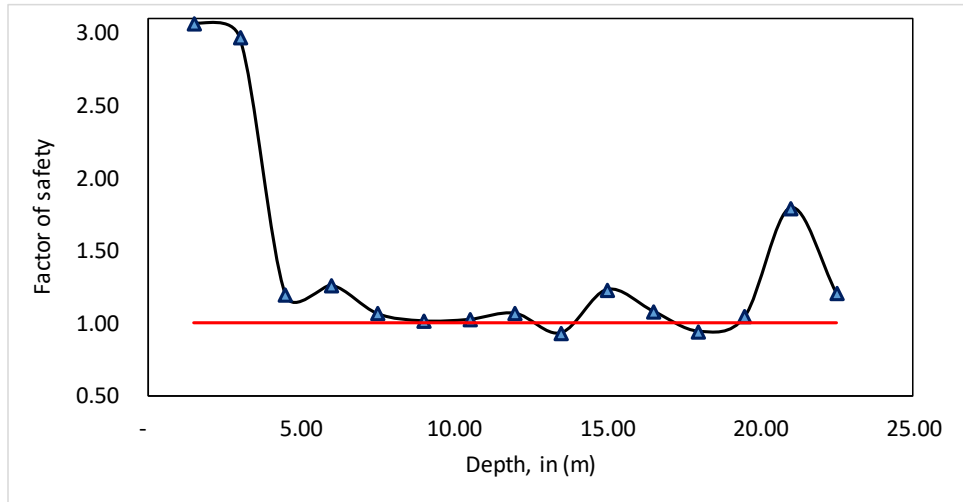


Fig 3.1 Depth V/s factor of safety by Youd and Idriss (2001) based on SPT ‘N’ Values

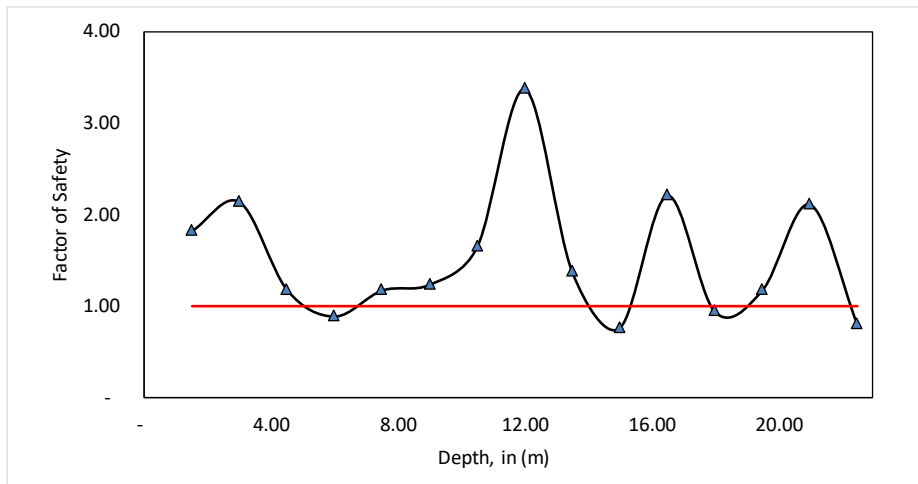


Fig 3.2 Depth V/s factor of safety by IS Code 1893 (Part1):2016 based on SPT ‘N’ Values

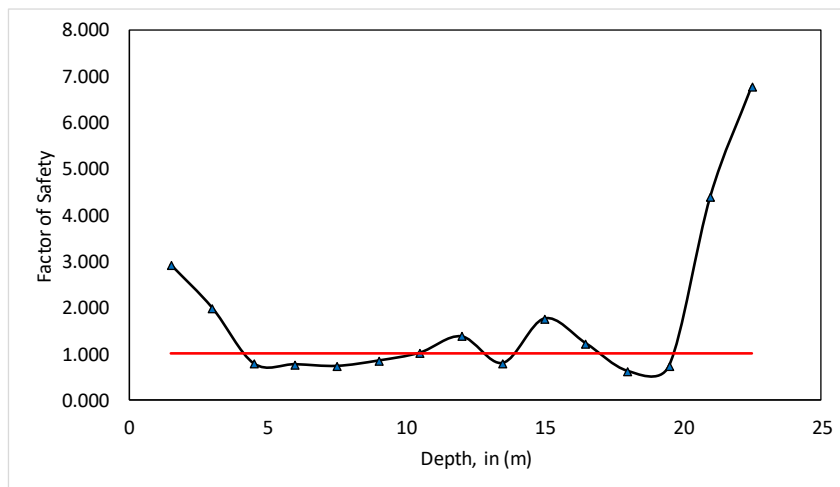


Fig 3.3 Depth V/s factor of safety by Idriss and Boulanger (2010) based on SPT ‘N’ Values

(3) In Table 3.1 Factor of safety from different analytical methods are presented, showing the difference in FOS value at various depth due to change in formulation of CSR (cyclic resistance ratio) and CRR (cyclic resistance ratio).

Table 3.1 Obtained FOS from different analytical methods

| Idriss and Boulanger (2010) | | | IS Code 1893 (Part1):2016 | | | Youd and Idriss (2001) | | |
|------------------------------------|------------|-------------------------|----------------------------------|------------|-------------------------|-------------------------------|------------|-------------------------|
| CSR | CRR | Factor of Safety | CSR | CRR | Factor of Safety | CSR | CRR | Factor of Safety |
| 0.156 | 0.458 | 2.930 | 0.154 | 0.281 | 1.822 | 0.154 | 0.468 | 3.06 |
| 0.215 | 0.429 | 1.995 | 0.152 | 0.326 | 2.136 | 0.152 | 0.447 | 2.96 |
| 0.245 | 0.195 | 0.796 | 0.168 | 0.197 | 1.175 | 0.151 | 0.177 | 1.19 |
| 0.263 | 0.205 | 0.779 | 0.191 | 0.169 | 0.887 | 0.154 | 0.191 | 1.25 |
| 0.275 | 0.205 | 0.743 | 0.207 | 0.243 | 1.171 | 0.172 | 0.180 | 1.06 |
| 0.284 | 0.243 | 0.858 | 0.219 | 0.270 | 1.234 | 0.185 | 0.185 | 1.01 |
| 0.292 | 0.301 | 1.029 | 0.221 | 0.365 | 1.647 | 0.190 | 0.192 | 1.02 |
| 0.303 | 0.418 | 1.381 | 0.220 | 0.742 | 3.372 | 0.191 | 0.201 | 1.06 |
| 0.309 | 0.249 | 0.808 | 0.216 | 0.296 | 1.371 | 0.190 | 0.175 | 0.93 |
| 0.322 | 0.569 | 1.768 | 0.211 | 0.160 | 0.760 | 0.187 | 0.227 | 1.23 |
| 0.327 | 0.402 | 1.232 | 0.204 | 0.451 | 2.208 | 0.183 | 0.195 | 1.08 |
| 0.325 | 0.207 | 0.637 | 0.196 | 0.184 | 0.938 | 0.176 | 0.163 | 0.94 |
| 0.332 | 0.246 | 0.740 | 0.188 | 0.220 | 1.171 | 0.169 | 0.174 | 1.04 |
| 0.364 | 1.607 | 4.411 | 0.179 | 0.377 | 2.111 | 0.162 | 0.286 | 1.79 |
| 0.379 | 2.572 | 6.796 | 0.169 | 0.135 | 0.798 | 0.153 | 0.182 | 1.20 |

CHAPTER 4

4.1 Methodology Adopted To Calculate V_s

MASW is abbreviated as Multichannel Analysis of Surface Waves Park et al. (1999), was first who introduced this seismic exploration method. It evaluates ground stiffness by determining subsurface shear wave velocity (V_s) in one-Dimensional, two-Dimensional, and three-Dimensional for the use of soil engineering applications in the 0-30 meter depth range.

MASW measures seismic surface waves caused by different kinds of seismic sources, such as a sledge hammer, investigations their distribution velocities, and afterwards concludes shear-wave velocity (V_s) deviations below the examined area that are most effective for the analysed distribution velocity pattern of surface waves. Shear wave velocity, which is one of the elastic constants, is nearly correlated to Young's and shear modulus. V_s is a soil parameter that give instant ground stiffness and is hence frequently used to determine load-bearing capacity.

4.2 Types of Seismic Waves

Seismic Waves: - There are two types of seismic waves produced when an earthquake occurs: body waves and surface waves. Seismographs record the energy produced by seismic waves which flows through the earth. Seismic waves are of two types described as below:

4.2.1 Body Waves: Body waves reached on ground surface before the surface waves created by an earthquake because they go through the interior of the ground. The frequency of these waves is more than from surface waves. These waves are of two types.

1. Primary Waves: primary, compressional or longitudinal waves are other names for these waves. They are comparable to sound waves in that the motion of a single particle

traveling through a primary-wave is parallel to the direction of travel. Alike sound Waves, primary-waves can travel in solids and fluids.

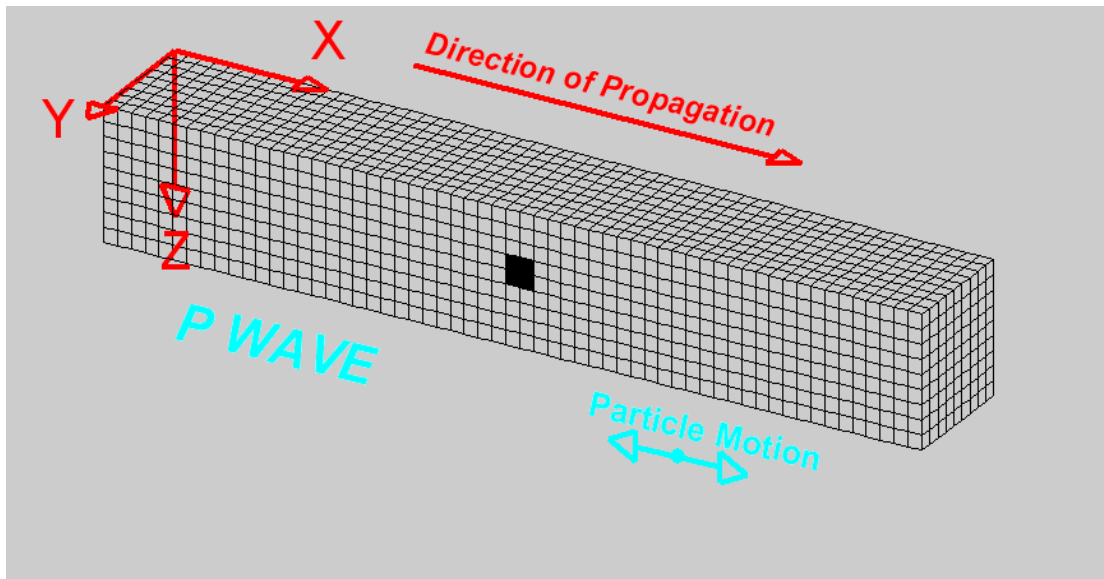


Fig 4.1 Propagation of Primary/Compressional Wave

2. S Waves: Secondary, shear, or transverse waves are other names for these waves. When they flow through a medium, they generate shear distortions. The movement of a individual particle in Secondary waves is perpendicular to the direction of Secondary-wave travel. Material like Fluids, which do not have any shearing strength, unable to maintain s-wave. S-waves can be divided into two parts based on particle movement direction SV waves, which appear on the vertical and radial components of seismographs, and SH waves, which occur on the tangential component.

The stiffness of the materials through which body waves travel influences their speed. Other seismic waves travel slower than primary-waves. because geologic materials are stiffest in compression, hence they are the first to arrive at a certain location.

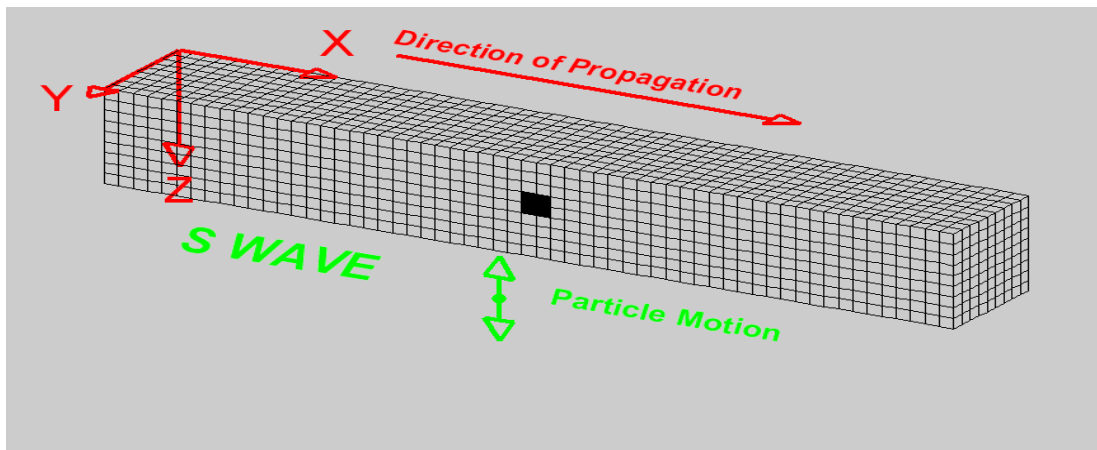


Fig 4.2 Propagation of Secondary/Shear Wave

4.2.2 Surface Waves: These are the waves which are generated when body waves combined with the surficial deposits of the earth. They are travelling alongside the earth's surface and their amplitude decreases with depth due to this they always arrived after the occurrence of body waves for the earthquakes destruction/damage, surface waves are mostly responsible. Surface wave are of two types:

1. Love Waves: love waves moves similar to the S – waves but they don't have a vertical displacement SH-waves combined with a soft surficial layer to generate love waves, which have no vertical particle motion component.

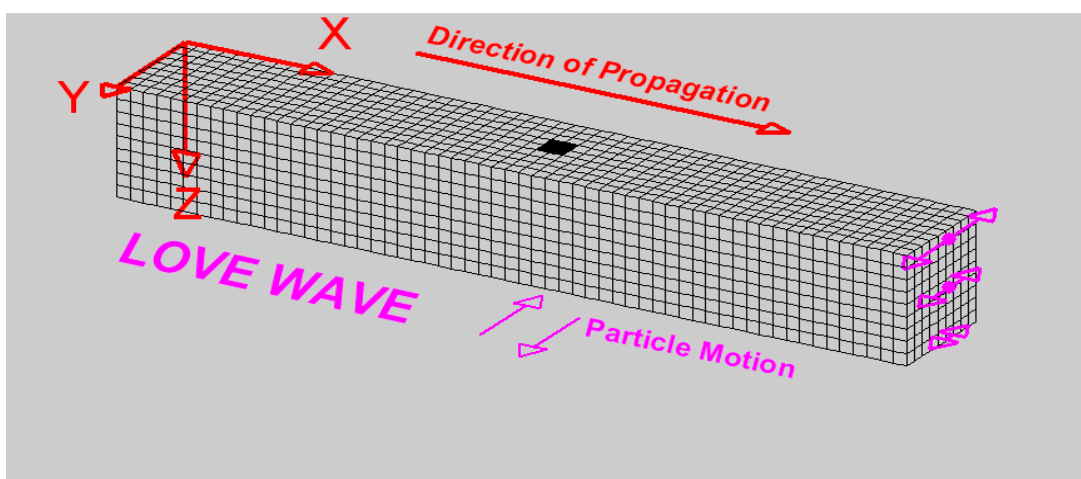


Fig 4.3 Propagation of Love Wave

2. Rayleigh Waves: John William Strutt, Lord Rayleigh has discovered this surface waves called Rayleigh wave, these are created when p waves interact with SV waves on the ground surface, causing particle movement both vertically and horizontally. It causes

the ground to move in the same direction as the wave, up and down as well as side to side. They travel in a same manner, as the waves generated into a pond when we through a rock in it. Rayleigh waves are travel slower than the other types of waves, they travel around at a 10 % lower speed that secondary type body waves

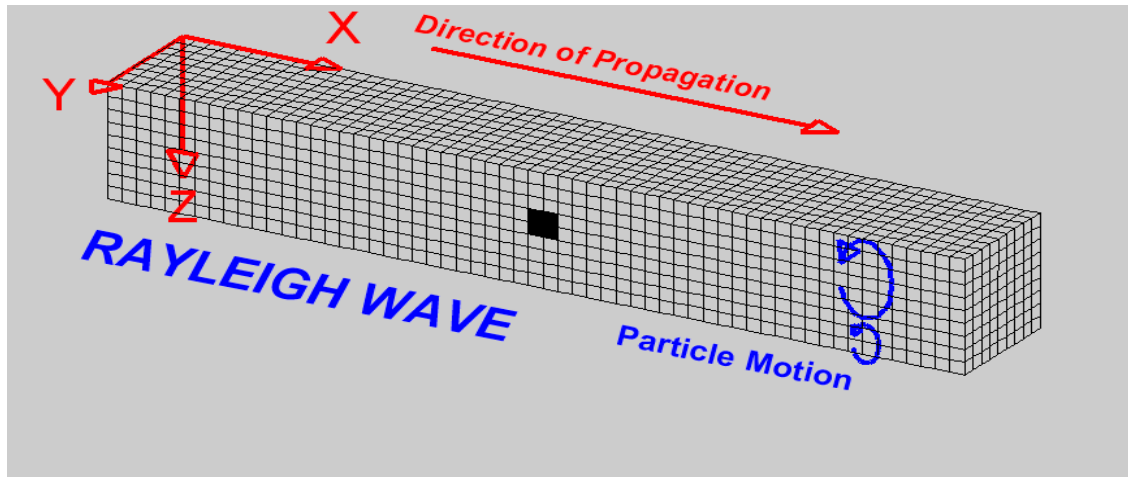


Fig 4.4 Propagation of Rayleigh Wave

4.3 Instruments Setup

4.3.1 Seismograph

The seismograph is a device that records the voltages of input geophones in a timed sequence. Digital seismographs are required for stacking, analysing, and archiving enormous amounts of data. The seismograph is capable of detecting the source, receiving digital geophone signals, storing multichannel data, and displaying certain processing results. Seismic data in the present work were recorded using Gea24 seismograph. Gea24 can be placed either at the ends or in the center of the spreading, in the present work we were conducted while keeping the seismograph in the Centre of the cables. Table 4.1 shows the technical specifications of the GEA24 seismograph which was used for stacking the data.



Fig 4.5 Seismograph

Table 4.1 Shows the technical specifications of the instrument GEA24 used

| | |
|-----------------------|--|
| Number of channels | 24 ⁺ trigger |
| Sampling Interval | Active up to 125 microsec on 24 channels |
| Acquisition Length | 27500 samples@24 channels |
| Stackings | Unlimited number of stackings |
| Trigger | Normally closed contact |
| Geophone Frequency | 4.5 Hz |
| Noise Monitor | All channels + trigger |
| Data Format | SEG2,SAF |
| Operating Temperature | -30°C to +80°C |
| Dimension | 24cm x 19.5cm x 11cm |
| Weight | 2 Kg |

4.3.2 Geophones:

Geophones are devices that detect ground vibrations. Geophones, also known as seismometers or detectors, measure seismic energy coming at the ground's surface. The modern geophones are a moving coil electromagnetic type. Figure 4.6 shows a schematic diagram and a field shot of the movable spiral electromagnetic geophones. Inside geophones a magnet in the shape of a cylinder with two circular grooves carved into it. It consist a coil of very tiny wire with a large number of twists is suspended centrally in the slot. Importance of Geophone frequency F_G explained in the below:



Fig 4.6 Geophones

Importance of Geophone Frequency (F_G):

- Lowest frequency (f_{\min}) can be found by F_G i.e. $f_{\min} \approx F_G$
- Longest wavelength (λ_{\max}) can be found by f_{\min} :
- $\lambda_{\max} = V_{\max}/f_{\min} \approx V_{\max}/F_G$ (V_{\max} = maximum phase velocity calculated)
- Hence (Z_{\max}) maximum exploration depth of MASW analysis can be found by F_G :
- $Z_{\max} \approx 1/2 \lambda_{\max} \approx 1/2 V_{\max}/F_G$

Table 4.2 Geophone frequency and their possible investigation depth

| Geophone frequency F_G | Max. Investigation Depth(Z_{\max}) |
|--------------------------|--|
| ≥ 100 Hz | ≤ 5 m |
| 30 - 100 Hz | ≤ 10 m |
| 10 - 30 Hz | ≤ 20 m |
| 4 - 10 Hz | ≤ 30 m |
| 1 - 4 Hz | ≤ 100 m |

4.3.3 Sledge Hammer

A 10 kg sledge hammer with an aluminium plate was utilised as a source that released greater energy in the ground at lower frequencies. Its impact energy is proportional to the wavelength range of the produced surface waves, which is used to govern the maximum depth of investigation. The sledge hammer and aluminium plate are Shown in fig 4.7. How the energy of striking of hammer is depend on investigation depth is explained in fig. 4.8.



Fig 4.7 Sledge Hammer

4.3.4 Location of MASW Testing

Below figure 4.8 shows the location where we have setup the MASW these are the approximately same location where the bore hole test had been done showed in DTU soil report. The soil is classified as a sandy silt for initial 6m and silty sand for depth up to 30 m from the ground level according to IS 1498- 1970 with different values of shear parameters along with the depth (Soil Test Report). In this study the bore hole test data has been taken from the DTU soil report in which is done by Allied Engineers 2 Year back at 28°44'54'' N and 77°07'09''E. The bearing capacity of soil is calculated analytically as classical approach using IS 2131-1981, IS 6403-1981, IS 1904-2006 and IS 8009 Part 1-1976, considering both permissible settlement and shear failure criteria. While calculating bearing capacity under shear failure criteria, local shear failure of soil is assumed, gives less bearing capacity value as compared to general shear failure, making the whole approach on a safer side.

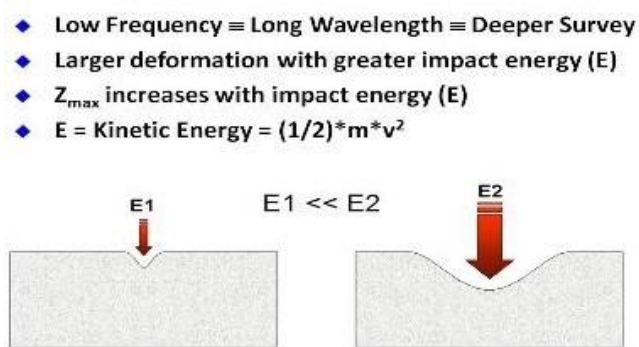


Fig. 4.8 Effect of frequency and energy on investigation depth



Fig 4.9 Location of Masw Testing

Table 4.3 Calculated Shear Wave Velocity Vs30

| Site | Station Code | Vs (m/sec) |
|------------|-------------------|------------|
| Location 1 | BH 1, BH 2, BH 10 | 310 |
| Location 2 | BH 5, BH 8, BH 9 | 267 |
| Location 3 | BH 6, BH 7 | 315 |
| Location 4 | BH 3, BH 4, | 290 |

4.4 Data Acquisition and Analysis

This present study MASW method was used to collect and process the data at the four location near to bore location showed in the Delhi Technological University soil report to get the precise dispersion curve of waves and then the inversion process of these curve have been made by winMASW software which is developed by ElioSoft.

The initial stage in the analysis is to create a list that includes all waveform files as well as the source receiver setup. Vs30 is the average shear wave velocity over the top 30

meters of soil, and it is calculated by dividing 30 meters by the travel time from the surface to 30 meters, as stated in eq 4.1 (Satyam, D. N., and Rao, K. S. 2008)

$$V_{S30} = \frac{30}{\sum_{i=1,N} \frac{h_i}{V_i}} \quad (4.1)$$

In this study 24 channel Gea24 seismograph was used for the seismic refraction and MASW testing. This is extremely proficient digital seismograph with very light mass and low power requirement. Twelve geophones of 4.5 frequency which are connected on either side to the seismograph with connecting cables as shown above. In this study 24 geophones were laid out in a linear length of 2m spacing were connected to the seismograph. So total survey length was 48m. A trigger geophone was also used to initialize the reading. Seismic Data for each shot was digitally recorded and save in the laptop as shown in Fig 4.14 and 4.15.

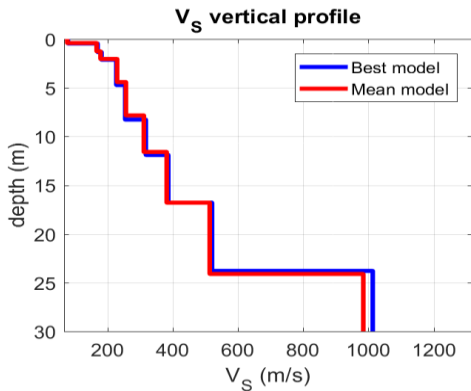


Fig 4.10 Location – 3

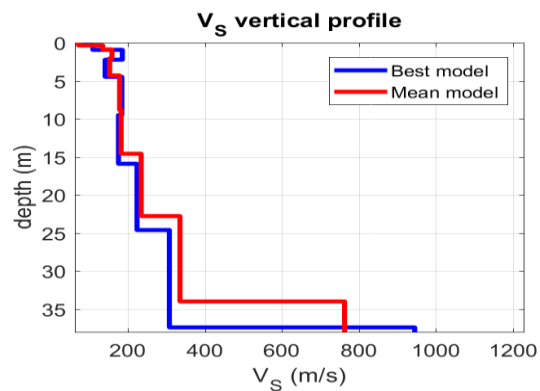


Fig 4.11 Location – 2

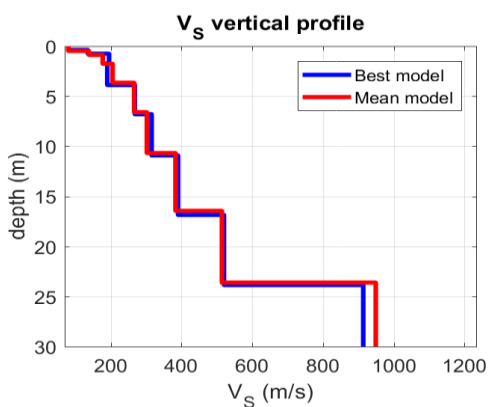


Fig 4.12 Location - 1

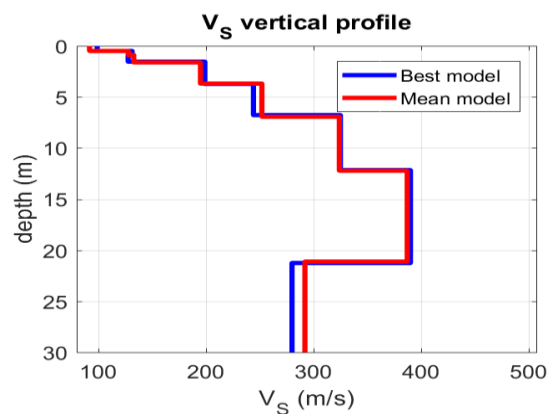


Fig 4.13 Location – 4

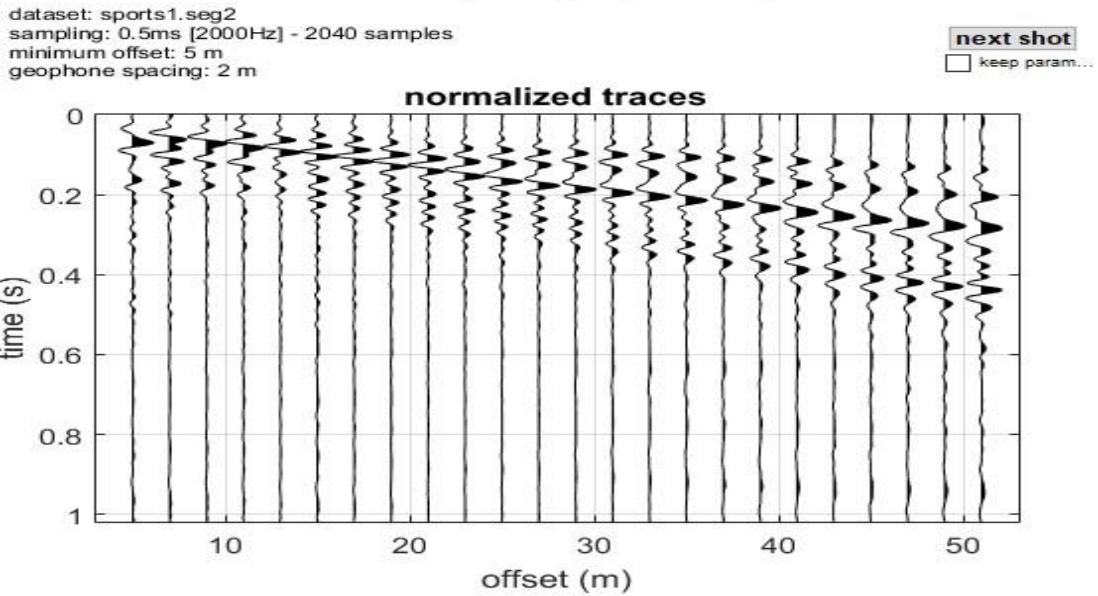


Fig 4.14 Location 1 Seismic Data

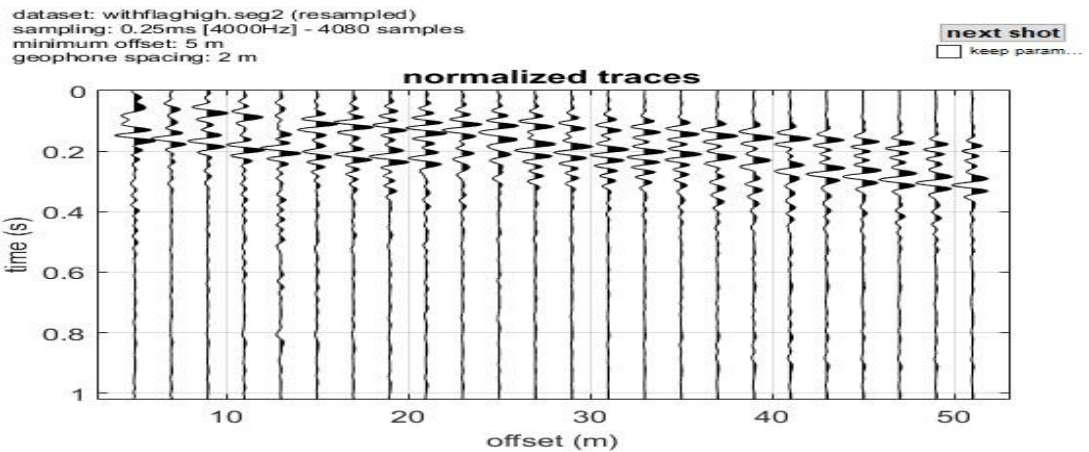


Fig 4.15 Location 3 Seismic Data

4.4.1 Analysis of data

Acquired surface wave seismic data was moved to the computer and it is processed using WINMASW software developed by Eliosoft. The many phases in data processing began with gathering the data into a single file in which all waveforms for each shot were recorded. The following step is to locate all pairs of traces that share a common mid-point (CMP) and calculate the cross correlation CMP collects.

Then the dispersion curves are generated by converting it into frequency domain for each correlation CMP gathers and then checked. Generation of a dispersion curve is one of the most critical steps for generating an accurate shear wave velocity profile. Dispersion curves are generally displayed as phase velocity versus frequency as shown in fig 4.16

and fig 4.17 respectively. The dispersion curve obtained from waveform data by nonlinear least square method is used to calculate the 1D shear wave velocity profiles shown in figs. 4.10 to 4.13 as same as the DTU soil bore data, here red colour shows the lower frequency means greater the wavelength by means of the below relation.

$$f = \frac{c}{\lambda} \quad (4.1)$$

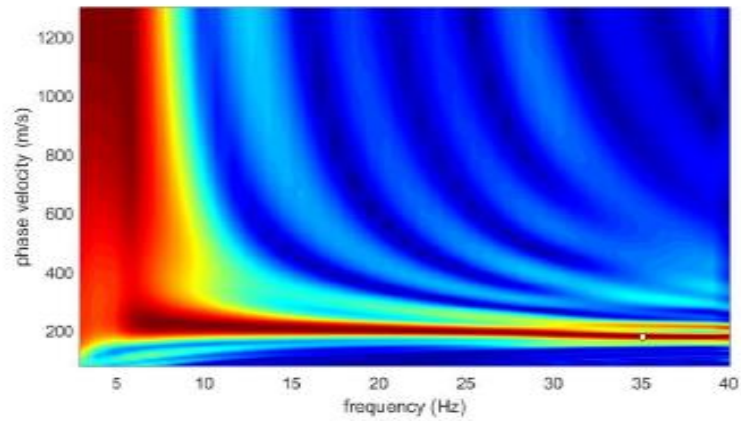


Fig 4.16 Location 1 Dispersion Curve

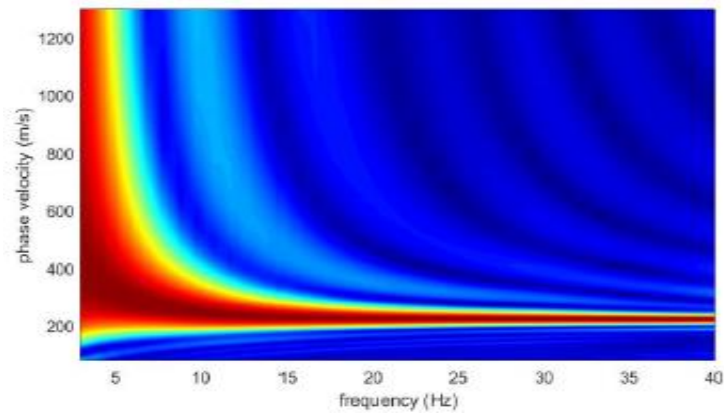


Fig 4.17 Location 3 Dispersion Curve

CHAPTER 5

5.1 Classical Approach

The ultimate bearing capacity, q_u , for a shallow isolated square footing with a depth denoted as D , a width denoted as B , and a length denoted as L , was calculated using the Plastic Equilibrium Concept. (Terzaghi, 1925) as given below

$$q_u = cN_c S_c + \gamma D N_q + 0.5 B N_\gamma S_\gamma \quad (5.1)$$

Where

a) Bearing capacity factors are

$$N_q = \exp(\pi \tan \phi) \tan^2(45^\circ + \phi/2) \quad (5.2)$$

$$N_c = (N_q - 1) \cot \phi \quad (5.3)$$

$$N_\gamma = 1.8(N_q - 1) \tan \phi \text{ by Hansen (1968)} \quad (5.4)$$

$$N_\gamma = (N_q - 1) \tan(1.4\phi) \text{ by Meyerhof (1956)} \quad (5.5)$$

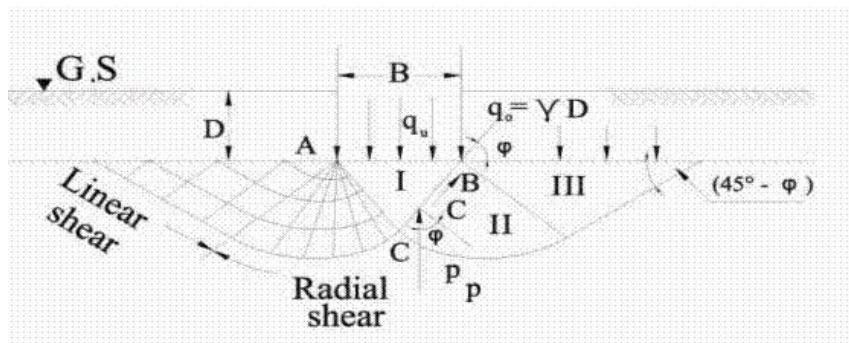


Fig 5.1 Zones of plastic equilibrium

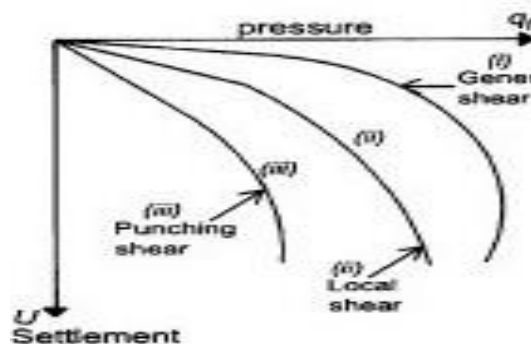


Fig 5.2 Modes of failure

b) Shape factors:

$$S_c = 1 + 0.20 B/L \dots\dots\dots(\text{for } \phi \neq 0 \text{ conditions}) \quad (5.6)$$

$$S_c = [1 + 0.20 B/L][1 + 0.3(D/B)^{0.25}] \dots\dots(\text{ for } \phi = 0 \text{ conditions, saturated clays}) \quad (5.7)$$

$$S_\gamma = 1 - 0.2 (B/L) \dots\dots\dots(B/L = \text{footing width to length ratio}) \quad (5.8)$$

$$S_\gamma = 0.6 \dots\dots\dots(\text{for circular footing}) \quad (5.9)$$

For an isolated square footing, the ratio of B/L shall be taken as 1, while for an isolated strip footing the ratio shall be taken as 0. The above formula can be applying only for shallow depth foundations when the depth of the footing D is less than the width of the footing B. The shape factors S_c' formula for saturated clays in undrained situations is presented above. , where ϕ is equal to 0 was given by (Skempton, 1951) using Nc curves. For Weak soil, or soil that is not dense or rigid enough, i.e relative density Dr is less than 0.35, spt blows value for 60% energy N60 is less than 8 , undrained cohesion C_u is less than 100 KPa, or shear wave velocity

V_s is more than 200 m/s, Equation (1) have to be modified by using lowered shear strength parameters C_r and ϕ_r in the place of the laboratory calculated C and ϕ , as given by (Terzaghi and Peck , 1967):

$$C_r = 0.67 * C \quad (5.10)$$

$$\tan \phi_r = 0.67 * \tan \phi \quad (5.11)$$

5.2 Approximations made in Classical Method

Approximations were taken in the determination of ultimate bearing capacity, q_u , which is used in equation (5.1) :

1. The soil was supposed and taken as totally homogenous and isotropic, despite the fact that real soil is extremely heterogeneous and anisotropic. Furthermore, the classical formula was created solely for a planar scenario, despite the fact that all footings are generally three-dimensional in reality.

2. The shear strength is shown in the first part of equation (5.1), the participation of the surcharge load caused by foundation depth is shown in the second part, and the self-weight is shown in the third part. In a stress-strain state which is non-linear, superimposing the multiple load scenarios is only an approximation.
3. The involvement of self-weight can only be estimated in terms of a rough estimate; Exact formulation is possible using numerical or graphical methods.
4. Soil shear strength above the footing's base level was not taken hence neglected.
5. There are three sorts of failure processes based on the compressibility of soil. (i) general shear, (ii) local shear, and (iii) punching shear (see Figure). The conjunctural concerns of Equation (5.1) only apply to the general shear failure, which is common in low compressibility soils like dense sands and stiff clays. When sufficient compression is exerted under the footing, an incomplete state of plastic equilibrium occurs in the local shear failure. Undeviating planar shear failures happen mostly accompanying vertical directions at each footing's edges in the punching shear failure, therefore Equation (5.1) is not valid for high-compressibility soils which may be having loose strata sand or a type of soft clay, which can develop as a result of local shear or punching shear failures. therefore, Equation (5.1) may only be used as a rough guide for such soils. In high compressibility soils, excessive settlement, rather than shear failure, is typically the limiting criterion.
6. Shear strength factors 1) cohesive force between particle 'C', 2) angle of internal friction when they are calculated in the laboratory from unbroken soil samples not always show the behavior of soil alike at site, are highly sensitive to the ultimate bearing capacity calculations. Maximum bearing capacity is determined unrealistically, when the angle of internal of friction ϕ of soil was calculated incorrect in the laboratory due to calculated higher value than actual value. The actual values of soil properties as internal angle of friction, unit weight, void ratio, overburden pressure, presence of voids, and other soil properties will not be same in samples.
7. In practice, after a complete geotechnical survey, a precise number for permissible bearing capacity q_a is allotted to a specific production site. Small differences in the sizes, shape, and depths of foundations at a specific site, on the other hand, are neglected, and in general practice same value of bearing capacity have been used in mostly foundation design and in all the engineering applications.
8. To put the value of permissible bearing capacity in safer side, a factor of safety of 2.5 to 3 is normally used, considering for non-accurate and approximations made in classical

method This factor of safety reflects the “inaccurate” and "ignorance" in finding actual world soil conditions.

9. Finally, while Section 2 gives some quantitative help, defining whether the soil is of the "strong" or "weak" type for the purposes of applying decreased (two-thirds) shear strength parameters in accord with Equation (5.10)

5.2.1 Practical Guidelines

Table 5.1 summarizes the varieties of permissible bearing capacities for diverse groups of cohesive and granular type soils based on the authors' practical experiences. Table 5.1 also includes the values of SPT counts N_{60} , shear strength parameters C_u , and, relative density D_r and shear wave velocity V_s for each soil type for comparison and quick reference. The permitted bearing pressures q_a are examined to ensure that they meet the empirical recommendations of the Building (Code, 1997) , the Turkish (Earthquake, 1998) Code.

Table 5.1. allowable bearing capacities (KPa) Building code (1997) variation for different soil type

| soil type | | N_{60} | C'_u | ϕ'_{av} | V_s | q_a (Kpa) | | | | | |
|-----------|---------------------------|----------|---------|--------------|----------|-------------|---------|---------|-----|-----|-----|
| No. | Cohesive soils | - | KPa | degree | m/s | 100 | 200 | 300 | 400 | 500 | 600 |
| 1 | Very soft clays and silts | 0-2 | 0-20 | 20 | 0-100 | 0-50 | | | | | |
| 2 | Soft clays and silts | 2-4 | 20-50 | 22 | 0-200 | 0-75 | | | | | |
| 3 | Medium stiff clays | 4-8 | 50-100 | 24 | 200-350 | 75-150 | | | | | |
| 4 | Stiff clays | 8-15 | 100-150 | 26 | 200-600 | 100-250 | | | | | |
| 5 | Very stiff clays,boulders | 15-30 | 150-200 | 28 | 450-800 | | 200-350 | | | | |
| 6 | Hard clays, boulders | 30-50 | 200-400 | 30 | 600-900 | | 250-400 | | | | |
| 7 | Very hard clays | 50-R | 400-600 | 30 | 800-1200 | | | 350-500 | | | |
| No. | Granular soils | N_{60} | D_r | ϕ'_{av} | V_s | | | | | | |
| 1 | Very loose sand | 0-4 | 0-20 | 28° | 0-100 | 0-50 | | | | | |
| 2 | Loose sand and gravel | 4-10 | 20-35 | 30° | 100-350 | 50-150 | | | | | |
| 3 | Medium dense sand,gravel | 10-30 | 35-65 | 32° | 250-700 | 100-300 | | | | | |
| 4 | Dense sand and gravel | 30-50 | 65-85 | 37° | 600-1100 | | 250-450 | | | | |
| 5 | Very dense sand gravel | 50-R | 85-99 | 40° | 800-1500 | | | 350-600 | | | |

C'_u = Undrained Cohesion (KPa), D_r = Relative Density (%), ϕ'_{av} = Avg Internal Friction Angle, V_s = Shear Wave Velocity (m/s), q_a = Allowable Bearing Capacity (KPa).

5.3. Allowable Bearing Capacity by Shear Wave Velocity

5.3.1 For the purpose of settlement control

The following formula can be used to calculate the allowed bearing capacity, q_a , below a shallow foundation in units KPa, which is derived after various case histories, as mentioned in the following steps:

$$q_a = 0.024 \gamma V_s \quad (5.12)$$

$$q_a = 2.4 (10^{-4}) \rho V_s \quad (5.13)$$

here, γ = soil unit weight (KN/m³) and v_s = shear wave velocity (m/sec). A high safety factor against the possible soil shear failures always require in suitable foundation design which is also ensure that settlement especially differential settlement limits given by Skempton and Macdonald (1956). Therefor the constant in the empirical formula given above decided to as lower side, safeguarding that no settlement problems will arise in practically soft soil. This issue has been thoroughly investigated and proven for all soft, "weak" soil conditions identified in Table (5.2) case studies. In spite the fact that the authors' empirical expressions for Equation (5.12) are based on comprehensive Geotechnical and Seismic soil tests at fourteen different locations, they shall be applied with carefulness. The permitted bearing pressure should also be determined using traditional methods employing Terzaghi's soil characteristics. For comparatively important structures, and mainly till the reliability of these simple expressions has been rigorously validated and adjusted over a considerable historical of time.

Using the presented empirical formulae, only the permitted bearing pressure can be determined. However, especially for soft soil conditions and big structures, settlement calculation should be done using the elastic theory given by (Skempton 1956) or the Skempton technique (1957). Because settlements might be the deciding factor at often.

5.3.2.For Setting an Upper Limit for q_a

For shear wave velocities value which is more than 500m/s. Through a factor sv , the empirical formula in Equation (5.12) is tweaked to provide steadily decreasing results. Particularly, especially for rocky formations, in order to define a reasonable top limit for the acceptable bearing capacity.

$$q_a = 0.024 \gamma V_s S_v \geq 30.6 \gamma \quad (5.14)$$

$$S_v = 1 - 3 \times 10^{-6} (V_s - 500)^{1.6} \quad (5.15)$$

Figure(5.3) shows the fluctuation of allowed bearing capacity q_a as a function of shear wave velocity v_s , where the factor s_v sets an fixed limit of $q_a = 30.6 * \gamma$ for shear wave velocity v_s is more than 2000 m/s to reduce bearing capacity.

Table 5.2 Locations of various case study (Tezcan ,2006) with their allowable bearing capacity

| No. | Building identity | Number of bore holes and average depth | | Footing depth D <i>m</i> | Number of Surveys | | Allowable bearing capacity, q_a , in Kpa | |
|-----|--|--|----------|-----------------------------|-------------------|-----|--|-----|
| | | <i>Number</i> | <i>m</i> | | (a) | (b) | (c) | (d) |
| 1 | Ataturk Primary School Building Babaeski, Kirklareli, | 2 | 15.30 | 4.00 | 2 | 2 | 281 | 287 |
| 2 | Residential Apartments Yesilcay Cooperative, Cay,Afyon | 4 | 9.50 | 2.50 | 3 | 3 | 110 | 147 |
| 3 | Zeki Ornek, Housing complex, Gokturk Village, Eyup, Istanbul | 2 | 20.00 | 3.00 | 1 | 3 | 150 | 203 |
| 4 | Oztas Apartments, Florya Senlik, Bakırkoy, Istanbul | 2 | 20.00 | 3.00 | 1 | 3 | 146 | 164 |
| 5 | Oil tanks, Haramidere, Istanbul | 3 | 8.00 | 2.50 | 3 | 3 | 165 | 113 |
| 6 | Oil tanks, Samsun,Black Sea | 6 | 25.00 | 2.50 | 3 | 2 | 215 | 224 |
| 7 | Oil tanks, Mudanya,Bursa | 4 | 20.7 | 2.50 | 3 | 3 | 100 | 133 |
| 8 | Oil tanks, Cubuklu,Istanbul | 3 | 12.00 | 1.00 | 3 | 4 | 115 | 100 |
| 9 | Oil tanks, Iskenderun | 5 | 5.50 | 1.50 | 3 | 3 | 520 | 374 |
| 10 | Oil tanks, Mersin | 8 | 26.10 | 2.50 | 3 | 3 | 187 | 218 |
| 11 | Oil tanks, Derince,Kocaeli | 7 | 21.00 | 1.50 | 3 | 3 | 110 | 86 |
| 12 | Oil tanks, Derince,Kocaeli | 7 | 21.00 | 7.00 | 3 | 3 | 222 | 205 |
| 13 | Oil tanks, Aliaga,Izmir | 6 | 19.20 | 2.50 | 3 | 4 | 231 | 234 |
| 14 | Suleyman Demirel University,Isparta, Southern Turkey | 2 | 12.00 | 4.00 | 2 | 2 | 120 | 124 |

Here a = seismic surveys no, b = geophysical survey no, c = allowable bearing capacity by

conventional method, d = allowable bearing capacity by shear wave velocity eq 5.12

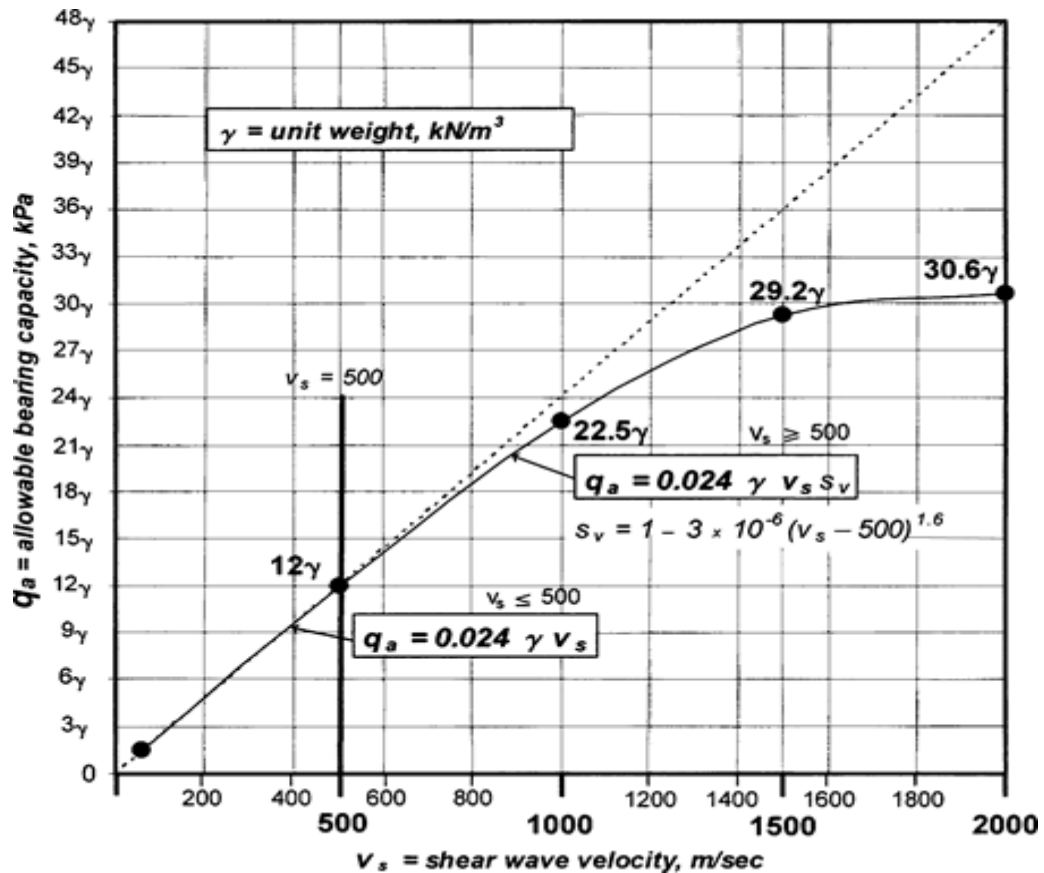


Fig 5.3 Allowable bearing capacity of soils relation with V_s

5.4 To Determine Unit Weights

A direct relationship exists between a soil layer's unit weight and Primary-wave velocity. The authors propose the following empirical correlation in this regard, by extensive laboratory testing case histories:

$$\gamma_p = \gamma_0 + 0.002v_p \quad (5.16)$$

Here γ_p = unit weight (KN/m³) as a function of primary wave velocity, v_p = primary wave velocity (m/s), γ_0 = unit weight for the reference.

$\gamma_0 = 16$ for loose sandy, silty and clayey soils

$\gamma_0 = 17$ for dense sand and gravel

$\gamma_0 = 18$ for mudstone, limestone, conglomerate etc.

$\gamma_0 = 20$ for tuff, greywacke, sandstone, schist etc.

As we can see in the below fig (5.4), the unit weights can easily be evaluated by the empirical formula given above in equation (5.16) are given plausible result comparison

to the calculated unit weights in the laboratory, the expression gives the exact approximation values for the different types of soils when we have the primary wave velocity calculated by seismic techniques. This is the very quick and easiest way to evaluate the unit weights rather to take the soil sample helps us to find the allowable bearing capacity for different types of soil by the given equation (5.12) above.

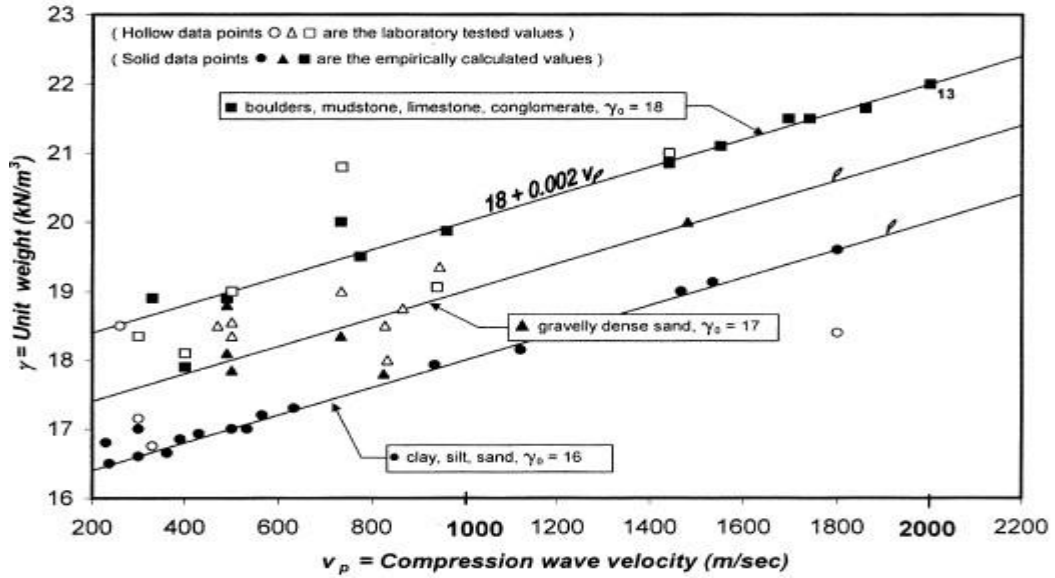


Fig 5.4-unit weight relation to v_p

CHAPTER 6

6.1 Evaluation of Allowable Bearing Capacity

A series of case studies have been examined for the purpose of develop a comprehensive and consistent relation between the permissible bearing capacity q_a and the shear wave velocity v_s , as represented in Table (5.2). Similarly, In this study I have evaluated the insitu shear wave velocity for Delhi technological university soil profile by using the MASW Seismic method to compare the allowable bearing capacity of University soil which was determined earlier as shown in fig 6.1 to 6.4. however, If we have the several values for the individual soil characteristics in the particular layer from the bore holes data, also when we do seismic data acquisition there may be the chances to get the same data we get to the nearby borehole so in that case we just to take the average of those different parameters which we got in the field.

6.2 Using of Classical Method to Calculate allowable bearing capacity

The first part of the below figure evaluated allowable bearing capacity for different bore hole location by choose significant soil parameters evaluated in the bore hole drill of delhi technological university. The parameters have choosen are shape factors depend on the value of anlge of internal friction, unit weight(KN/m^3). In the calculation of bearing capacity shear strength parameters have been reduced up to $2/3$ times due to consider the local shear failure in instead of general shear failure as given in equation (5.10 and 5.11).

6.3 Use of V_s to Evaluate Allowable bearing capacity

The second part contain in situ evaluated v_s (m/sec), soil weight density (KN/m^3), and q_a = permissible bearing capacities (Ton/m^2) calculate by shear wave velocities, by using of equation (5.12). Semih S. Tezcan (2006). The insitu shear wave velocity v_s , have been calculated by the using of Rayleigh wave velocities dispersion curve using the seismic method called MASW. The transmitting waves have been noted with the help of 24-geophone/channels.

| DEPTH (m) | SUB SOIL PROFILE | SOIL DESCRIPTION AND CLASSIFICATION | By Classical theory Eq.1 | By Shear wave velocity Eq.3 |
|-----------|------------------|--|--------------------------|-----------------------------|
| 0.00 | | Brownish Colour Inorganic Silty Clay (CL) | $N_c' = 14.78$ | $V_s = 290$ |
| 3.00 | | Inorganic Clayey Silt (ML-CL) | | |
| 6.00 | | Inorganic Silty Sand (SM) | $N_q' = 6.35$ | |
| 13.00 | | Inorganic silty Clay (CL) | $N_y' = 5.33$ | $Y = 19$ |
| 18.00 | | Inorganic Clayey Silt (ML-CL) | $q_b = 11.78$ | $q_b = 13.23$ |
| 23.00 | | Inorganic Silty Sand (SM) | | |
| 26.00 | | Inorganic silty Clay (CL) | | |
| 30.00 | | | | |

Fig 6.1 Allowable bearing capacity Location 4

| DEPTH (m) | SUB SOIL PROFILE | SOIL DESCRIPTION AND CLASSIFICATION | By Classical theory Eq.1 | By Shear wave velocity Eq.3 |
|-----------|------------------|--|--------------------------|-----------------------------|
| 0.00 | | Brownish Colour Inorganic Silty sand (ML) | $N_c' = 14.43$ | $V_s = 310$ |
| 2.5 | | Inorganic Silty Sand (SM) | | |
| 19.00 | | Inorganic Silty Sand (SM) | $N_q' = 6.12$ | $Y = 17.3$ |
| 21.00 | | Inorganic Silty Sand (SM) | $N_y' = 5.05$ | $Y = 17.3$ |
| 30.00 | | | $q_b = 10.53$ | $q_b = 12.87$ |

Fig 6.2 Allowable bearing capacity Location 1

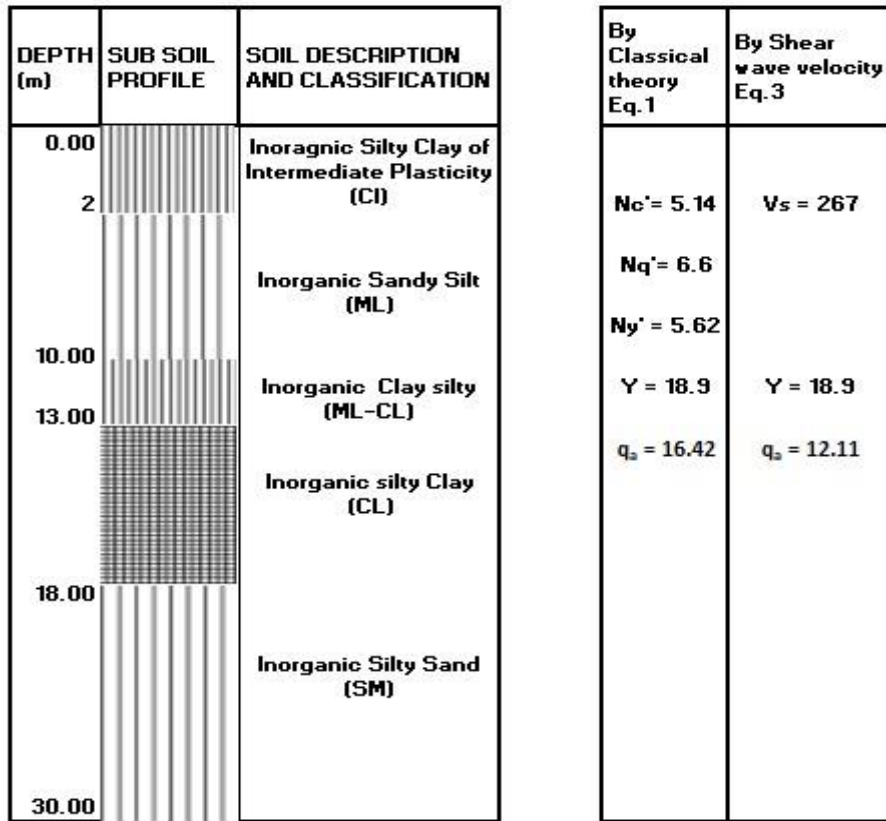


Fig 6.3 Allowable bearing capacity Location 2

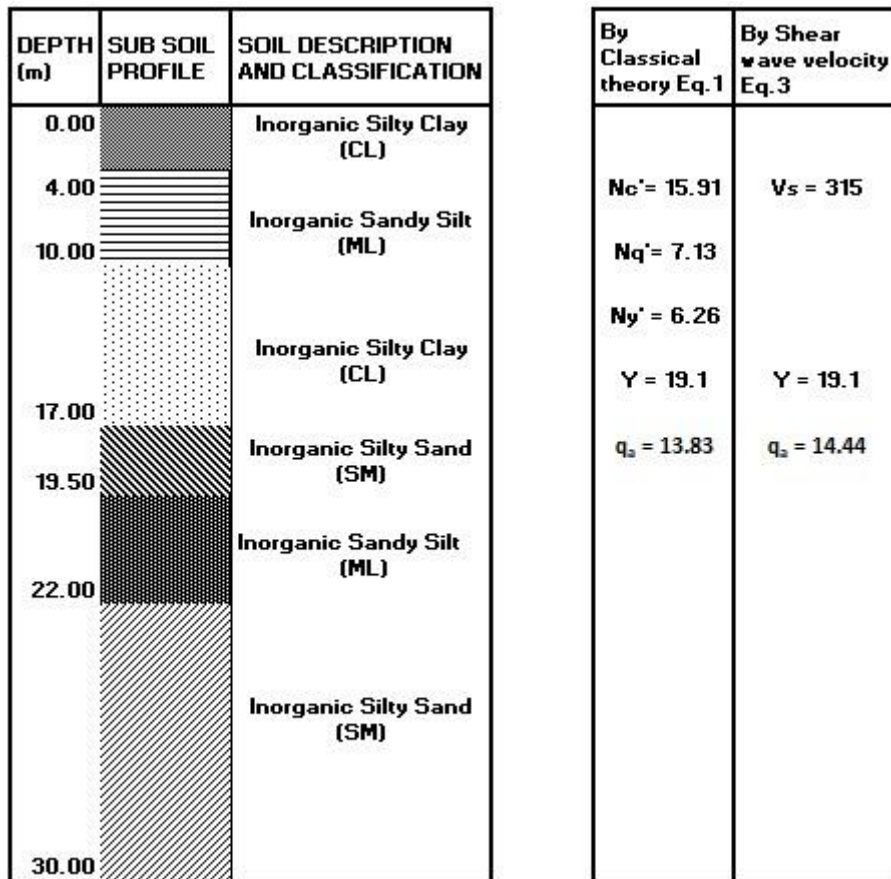


Fig 6.4 Allowable Bearing Capacity Location 3

CHAPTER 7

7.1 CONCLUSION

The major conclusion attained from the above study is emphasized as follows:

- 1) Different methods for liquefaction potential assessment are analyzed, obtained different results due to the following factors: (i) Magnitude Scaling Factor, (ii) Different Cyclic Resistance Ratio formulas, (iii) Difference in CSR Cyclic Stress Ratio formula as shown in Table 3.1.

- 2) Evaluation of allowable bearing capacity is done using dispersion curves obtained from Winmasw software, useful where the SPT test is not feasible. Bearing capacity of soil is found in good agreement with the result obtained from theoretical approach with change of 22.22 %, 26.24 %, 12.3 %, 4.4 % for location 1, 2, 3 and 4 respectively.

- 3) The V_s values obtained for location 1, 2, 3 and 4 are 310 m/s, 267 m/s, 315 m/s and 290 m/s respectively. The V_s values are influenced by different soil deposit and also influenced by the external disturbances at the time of data acquisition.

- 4) The picking of frequency in the dispersion curve is very crucial step in processing of seismic data for obtaining the velocity profile curves also the noise reduction shall be properly apply to get the accurate Rayleigh wave velocity.

REFERENCES

- [1] Cetin, K. O., and Seed, R. B. (2004). "Nonlinear shear mass participation factor (rd) for cyclic shear stress ratio evaluation." *Soil Dynamics and Earthquake Engineering*, Elsevier, 24: 103-113.
- [2] DeBeer, E. E. (1970) Experimental determination of the shape factors and the bearing capacity factors of sand, *Geotechnique*, 20, 387–411.
- [3] Duffy, B.D., 2008, Development of Multi-channel Analysis of Surface Waves (MASW) for characterising the internal structure of active fault zones as a predictive method of identifying the distribution of ground deformation: Unpublished master's thesis, University of Canterbury, Christchurch, New Zealand.
- [4] Gautam, R., Shrivastava, A.K., Gupta, S., Sharma, V., (2020), In situ shear wave velocity from multichannel analysis of surface waves (MASW) tests at six sites of Delhi Technological University, International conference on innovative advancement in engineering and technology, (IAET-2020).
- [5] Hansen, J. B. (1968) *A Revised Extended Formula for Bearing Capacity*, Danish Geotechnical Institute Bulletin, No. 28.
- [6] H. B. Seed, and I. M. Idriss, "Simplified Procedure for Evaluating Soil Liquefaction Potential," *J. Soil Mechanics and Foundations Div.*, ASCE, 97:SM9, 1249-1273, 1971.
- [7] Idriss, I. M., and Boulanger, R. W. (2010). "SPT-based liquefaction triggering procedures." Rep. UCD/CGM-10/02, Dept. of Civil and Environmental Engineering, Univ. of California, Davis, CA.
- [8] Idriss, I. M. (1999). An update to the Seed-Idriss simplified procedure for evaluating liquefaction potential, in *Proceedings, TRB Workshop on New Approaches to Liquefaction*, Publication No. FHWA RD-99-165, Federal Highway Administration, January.
- [9] Idriss, I. M., and Boulanger, R. W. (2008). *Soil liquefaction during earthquakes*. Monograph MNO-12, Earthquake Engineering Research Institute, Oakland, CA, 261 pp.
- [10] Idriss, I. M., and Boulanger, R. W. (2004). Semi-empirical procedures for evaluating liquefaction potential during earthquakes, in *Proceedings, 11th International Conference on Soil Dynamics and Earthquake Engineering, and 3rd International*

Conference on Earthquake Geotechnical Engineering, D.Doolin et al., eds., Stallion Press, Vol. 1, pp. 32–56

- [11] Idriss, I.M., Boulanger, R.W.: Semi-empirical Procedures for Evaluating Liquefaction Potential during Earthquakes. *Soil Dyna. and Earth. Engg.* 26, 115--130 (2006).
- [12] IS 1893 Part-1, 2016, "Criteria for Earthquake Resistant Design of Structures, Annex F, p.38-42".
- [13] IS 1904-1986, "Code of Practice for Design and Construction of Foundations in Soils: General Requirements".
- [14] IS 2131-1981, "Method for Standard Penetration Test for Soils".
- [15] IS 6403-1981, "Code of Practice Determining of Bearing Capacity of Shallow Foundations".
- [16] IS 8009 Part-1, 1976, "Shallow Foundation Subjected to Symmetrical Static Vertical Loads.
- [17] IS 1498-1970, "Classification and Identification of Soils for General Engineering Purposes".
- [18] Kuribayashi, E. and Tatsuoka, F. (1975), "Brief Review of Soil Liquefaction during Earthquakes in Japan", *Soils and Foundations*, 15, 4, pp.81-92.
- [19] Kramer, L. S., (1996). "Geotechnical Earthquake Engineering", Prentice-Hall International series, ed William J. Hall.
- [20] Meyerhof, G. G. (1956) Penetration tests and bearing capacity of cohesionless soils, *Proceedings ASCE*, 82, (SM1), Paper 866, 1–19.
- [21] Park, C. B., Miller, R. D., and Xia, J. (1999). "Multi-channel analysis of surface waves." *Geophysics*, 64(3), 800-808.
- [22] Park, C.B., and Miller, R.D., 2006, Roadside passive MASW: Proceedings of the SAGEEP, April 2-6, 2006, Seattle, Washington.
- [23] Prandtl, L. (1921) U'ber die Eindringungsfestigkeit (Ha'rte) plastischer Baustoffe und die Festigkeit von Schneiden, (On the penetrating strengths (hardness) of plastic construction materials and the strength of cutting edges), *Zeit. Angew. Math. Mech.*, 1(1), 15–20.
- [24] Reissner, H. (1924) Zum Erddruckproblem (Concerning the earth-pressure problem), *Proc. 1st Int. Congress of Applied Mechanics*, Delft, pp. 295–311.
- [25] Satyam, D. N., and Rao, K. S. (2008). Seismic site characterization in Delhi region using multi-channel analysis of shear wave velocity (MASW) testing. *Electronic Journal of Geotechnical Engineering*, 13, 167-183.

- [26] Seed, H. B., and Idriss, I.M. (1971). “Simplified procedure for evaluating soil liquefaction potential.” *J. Soil Mech. Found. Div.*, 97(SM9), 1249–1273.
- [27] Seed, H. B., Tokimatsu, K., Harder, L. F. Jr., and Chung, R. (1985). “Influence of SPT procedures in soil liquefaction resistance evaluations.” *J. Geotech. Eng.*, 111(12), 1425–1445.
- [28] Seed, H. B., Tokimatsu, K., Harder, L. F. Jr., and Chung, R. (1984). The influence of SPT procedures in soil liquefaction resistance evaluations. Earthquake Engineering Research Center, University of California, Berkeley, Report No. UCB/EERC-84/15, 50 pp.
- [29] Sieffert, J. G. and Ch. Bay-Gress (2000) Comparison of the European bearing capacity calculation methods for shallow foundations, *Geotechnical Engineering, Institution of Civil Engineers*, 143, 65–74.
- [30] Skempton, A. W. (1951) The bearing capacity of clays, *Proceedings, Building Research Congress*, 1, 180–189
- [31] Skempton, A. W. and MacDonald, D. H. (1956) Allowable settlement of buildings, *Proceedings ICE*, 5(3), 727–768
- [32] Soil Test Report, Delhi Technological University.
- [33] Tezcan SS, Ozdemir Z, Keceli A. (2009). Seismic technique to determine the allowable bearing pressure for shallow foundations in soils and rocks. *Acta Geophys.* 57 (2):1–14. doi:10.2478/s11600-008-0077-z.
- [34] Terzaghi, K. (1925) Structure and volume of voids of soils, Pages 10, 11, 12, and part of 13 of *Erdbaumechanik auf Bodenphysikalischer Grundlage*, translated by A. Casagrande in *From Theory to Practice in Soil Mechanics*, John Wiley and Sons, New York, 1960, pp. 146–148.
- [35] Tezcan, S.S., Z. Ozdemir, and A. Keceli (2006), Allowable bearing capacity of shallow foundations based on shear wave velocity, *J. Geotech. Geol. Eng.* 24,203-218, DOI: 10.1007/s.10706-004-1748-4.
- [36] Vincent, P.D., Tsoflias, G.P., Steeples, D.W., and Sloan, S.D., 2006, Fixed-source and fixed-receiver walkaway seismic noise tests: A field comparison: *Geophysics*, Vol. 71, p. W41-W44
- [37] Xia, J., Miller, R.D., and Park, C.B., 1999, Estimation of near-surface shear-wave velocity by inversion of Rayleigh waves: *Geophysics*, v. 64, p. 691-700.
- [38] Youd, T.L., Idriss I.M., Summery Report on NCEER Workshop on Evaluation of Liquefaction Resistance of Soils, Nat. Ctr. for Earthquake Engg. Res., State Univ. of New

York, Buffalo (1997).

- [39] Youd, T. L., et al. (2001). “Liquefaction resistance of soils: Summary report from the 1996 NCEER and 1998 NCEER/NSF workshops on evaluation of liquefaction resistance of soils.” *J. Geotech. Geoenviron. Eng.*, 127(10), 817–833.